



**Calhoun: The NPS Institutional Archive**  
**DSpace Repository**

---

Theses and Dissertations

1. Thesis and Dissertation Collection, all items

---

1994

Mach number, flow angle, and loss  
measurements downstream of a transonic  
fan-blade cascade

Austin, Jeffrey G.

Monterey, California. Naval Postgraduate School

---

<http://hdl.handle.net/10945/30868>

---

This publication is a work of the U.S. Government as defined in Title 17, United States Code, Section 101. Copyright protection is not available for this work in the United States.

*Downloaded from NPS Archive: Calhoun*



Calhoun is the Naval Postgraduate School's public access digital repository for research materials and institutional publications created by the NPS community. Calhoun is named for Professor of Mathematics Guy K. Calhoun, NPS's first appointed -- and published -- scholarly author.

**Dudley Knox Library / Naval Postgraduate School**  
**411 Dyer Road / 1 University Circle**  
**Monterey, California USA 93943**

<http://www.nps.edu/library>

NAVAL POSTGRADUATE SCHOOL  
Monterey, California



# THESIS

MACH NUMBER, FLOW ANGLE, AND LOSS MEASUREMENTS  
DOWNSTREAM OF A TRANSONIC FAN-BLADE CASCADE

By  
Jeffrey G. Austin  
March 1994

Thesis Advisor:

Raymond P. Shreeve

Approved for public release; distribution is unlimited

Thesis  
A97145

NAVAL POSTGRADUATE SCHOOL  
MONTEREY CA 93943-5101

## REPORT DOCUMENTATION PAGE

Form Approved  
OMB No. 0704-0188

1a. REPORT SECURITY CLASSIFICATION <b>Unclassified</b>		1b. RESTRICTIVE MARKINGS	
2a. SECURITY CLASSIFICATION AUTHORITY		3. DISTRIBUTION/AVAILABILITY OF REPORT Approved for public release; distribution is unlimited	
2b. DECLASSIFICATION/DOWNGRADING SCHEDULE			
4. PERFORMING ORGANIZATION REPORT NUMBER(S)		5. MONITORING ORGANIZATION REPORT NUMBER(S)	
6a. NAME OF PERFORMING ORGANIZATION Naval Postgraduate School	6b. OFFICE SYMBOL (If applicable)	7a. NAME OF MONITORING ORGANIZATION Naval Postgraduate School	
6c. ADDRESS (City, State, and ZIP Code) Monterey, CA 93943-5000		7b. ADDRESS (City, State, and ZIP Code) Monterey, CA 93943-5000	
8a. NAME OF FUNDING/SPONSORING ORGANIZATION Naval Air Warfare Center Aircraft Division	8b. OFFICE SYMBOL PE-31 (If applicable)	9. PROCUREMENT INSTRUMENT IDENTIFICATION NUMBER N6237693WR00051	
8c. ADDRESS (City, State, and ZIP Code) P.O. Box 7176 Trenton, NJ 08628-0176		10. SOURCE OF FUNDING NUMBERS PROGRAM ELEMENT NO. WR024 PROJECT NO. 03 TASK NO. 001 WORK UNIT ACCESSION NO.	
11. TITLE (Include Security Classification) MACH NUMBER, FLOW ANGLE, AND LOSS MEASUREMENTS DOWNSTREAM OF A TRANSONIC FAN-BLADE CASCADE.(UNCLASSIFIED)			
12. PERSONAL AUTHOR(S) Austin, Jeffrey G.			
13a. TYPE OF REPORT Master's Thesis	13b. TIME COVERED FROM TO	14. DATE OF REPORT (Year, Month, Day) March 1994	15. PAGE COUNT 85
16. SUPPLEMENTARY NOTATION The views expressed in this thesis are those of the author and do not reflect the official policy or position of the Department of Defense or the U.S. Government.			
17. COCATH CODES FIELD GROUP SUB-GROUP		18. SUBJECT TERMS (Continue on reverse if necessary and identify by block number) Shock-Boundary Layer Interaction, Transonic Fan Simulation, Boundary Layer Separation	
19. ABSTRACT (Continue on reverse if necessary and identify by block number) Two dimensional flow measurements of Mach number and flow angle were conducted downstream of a transonic fan-blade cascade at a Mach number of 1.4 to provide baseline data for assessing the effect of vortex generating devices on the suction surface shock-boundary layer interaction. The experimental program consisted of the design and calibration of a traversing three-port pneumatic probe to measure Mach number and flow angle and initial cascade measurements to provide baseline data for the fully-mixed-out total pressure loss coefficient and flow turning angle. Similar tests are planned with the vortex generating devices installed. Comparisons with and without the vortex generating devices are needed to quantify the overall effect on the shock-boundary interaction in a transonic fan-blade passage, and to assess the potential for using vortex generating devices in military engine fans.			
20. DISTRIBUTION/AVAILABILITY OF ABSTRACT <input checked="" type="checkbox"/> UNCLASSIFIED/UNLIMITED <input type="checkbox"/> SAME AS RPT. <input type="checkbox"/> DTIC USERS		21. ABSTRACT SECURITY CLASSIFICATION Unclassified	
22a. NAME OF PERSONAL INDIVIDUAL Raymond P. Shreeve		22b. TELEPHONE (Include Area Code) (408) 656 - 2593	22c. OFFICE SYMBOL AA/SF

Approved for public release; distribution is unlimited.

Mach Number, Flow Angle, and Loss Measurements Downstream of a Transonic  
Fan-Blade Cascade

by

Jeffrey G. Austin  
Lieutenant, United States Navy  
B.S., University of Puget Sound, 1985


Submitted in partial fulfillment of the requirements for  
the degree of

MASTER OF SCIENCE IN AERONAUTICAL ENGINEERING


from the


NAVAL POSTGRADUATE SCHOOL  
March 1994

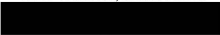
Author:

 Jeffrey G. Austin

Approved by:

 Raymond P. Shreeve, Thesis Advisor

 Garth V. Hobson, Second Reader

 Daniel J. Collins, Chairman,  
Department of Aeronautics and Astronautics

## ABSTRACT

Two dimensional flow measurements of Mach number and flow angle were conducted downstream of a transonic fan-blade cascade at a Mach number of 1.4 to provide baseline data for assessing the effect of vortex generating devices on the suction surface shock-boundary layer interaction. The experimental program consisted of the design and calibration of a traversing three-port pneumatic probe to measure Mach number and flow angle and initial cascade measurements to provide baseline data for the fully-mixed-out total pressure loss coefficient and flow turning angle. Similar tests are planned with the vortex generating devices installed. Comparisons with and without the vortex generating devices are needed to quantify the overall effect on the shock-boundary interaction in a transonic fan-blade passage, and to assess the potential for using vortex generating devices in military engine fans.

Thesis  
A 97145  
c.2

## TABLE OF CONTENTS

I.	INTRODUCTION .....	1
II.	EXPERIMENTAL DEVELOPMENTS.....	4
	A. PROBE DESIGN .....	4
	B. PROBE CALIBRATION.....	5
	1. Data Acquisition System.....	7
	2. Program of Measurements .....	7
	3. Probe Characteristics .....	8
	4. Application of the Calibration.....	11
	C. TRANSONIC CASCADE MODEL AND DATA ACQUISITION .....	12
	1. Transonic Cascade Model .....	12
	2. Data Acquisition System.....	14
III.	EXPERIMENTAL PROGRAM, RESULTS AND DISCUSSION .....	16
	A. EXPERIMENTAL PROGRAM .....	16
	B. REPEATABILITY TESTS.....	17
	C. TURNING ANGLE DISTRIBUTION .....	19
	D. PROBE STATIC PRESSURE DISTRIBUTION.....	20
	E. MODEL BASELINE MEASUREMENTS .....	21

IV. CONCLUSIONS AND RECOMMENDATIONS.....	30
APPENDIX A. PROGRAM "CAL_ACQ" .....	33
APPENDIX B. PROBE CALIBRATION RAW DATA .....	37
APPENDIX C. APPLICATION OF THE CALIBRATION.....	39
APPENDIX D. PROGRAM "NEW_READ_ZOC1" .....	46
APPENDIX E. MIXED-OUT LOSS CALCULATION .....	60
APPENDIX F. SELECTED RAW DATA.....	64
LIST OF REFERENCES .....	70
INITIAL DISTRIBUTION LIST.....	72

## LIST OF TABLES

TABLE 1.	PROBE CALIBRATION COEFFICIENTS.....	11
TABLE 2.	REPEATABILITY TESTS 2/24/94 RUN 2 AND RUN 4....	17
TABLE 3.	MEASURED PRESSURES AND PORTS ASSIGNED.....	22
TABLE 4.	PROBE TRAVERSE POSITION .....	22
TABLE 5.	BASELINE TUNNEL CONDITIONS .....	23
TABLE 6.	BASELINE FULLY-MIXED-OUT CONDITIONS .....	23
TABLE B1.	PROBE CALIBRATION RAW DATA X = 0.10 - 0.22.....	37
TABLE B2.	PROBE CALIBRATION RAW DATA X = 0.26 - 0.37.....	38
TABLE C1.	CALIBRATION METHOD RESULTS X = 0.10 - 0.22.....	44
TABLE C2.	CALIBRATION METHOD RESULTS X = 0.26 - 0.37.....	45

## LIST OF FIGURES

Figure 1.	Shock-Boundary Layer Interaction .....	1
Figure 2.	Low-Profile Vortex Generator .....	2
Figure 3.	Probe Tip Enlarged.....	4
Figure 4.	Free-Jet Calibration Apparatus.....	6
Figure 5.	Probe Holder Assembly .....	6
Figure 6.	Beta Characteristic .....	9
Figure 7.	Gamma Characteristic .....	9
Figure 8.	Wind Tunnel Facility.....	13
Figure 9.	Transonic Cascade Model Test Section .....	13
Figure 10.	Cascade Blading Geometry .....	15
Figure 11.	Blade Wake Survey: 2/24/94 Run 2.....	18
Figure 12.	Blade Wake Survey: 2/24/94 Run 4.....	18
Figure 13.	Angle Distribution Comparison.....	19
Figure 14.	Probe Static Pressure Distribution.....	21
Figure 15.	Baseline Blade Wake Survey: Run 1.....	24
Figure 16.	Baseline Blade Wake Survey: Run 2 .....	25
Figure 17.	Baseline Blade Wake Survey: Run 3 .....	26
Figure 18.	Baseline Blade Wake Survey: Run 4 .....	27
Figure 19.	Baseline Blade Wake Survey: Run 5 .....	28
Figure A1.	Program "CAL_ACQ" .....	33
Figure C1.	Pitch Angle vs. Gamma X = 0.1047.....	39
Figure C2.	Pitch Angle vs. Gamma X = 0.1397.....	39
Figure C3.	Pitch Angle vs. Gamma X = 0.1812 .....	40

<b>Figure C4.</b>	Pitch Angle vs. Gamma	X = 0.2192 .....	40
<b>Figure C5.</b>	Pitch Angle vs. Gamma	X = 0.2650 .....	41
<b>Figure C6.</b>	Pitch Angle vs. Gamma	X = 0.3002 .....	41
<b>Figure C7.</b>	Pitch Angle vs. Gamma	X = 0.3378 .....	42
<b>Figure C8.</b>	Pitch Angle vs. Gamma	X = 0.3698 .....	42
<b>Figure C9.</b>	X vs. Beta .....		43
<b>Figure D1.</b>	Program "NEW_READ_ZOC1" .....		46
<b>Figure E1.</b>	Fully-Mixed-Out Control Volume .....		60
<b>Figure F1.</b>	Run 2 2/24/94 Raw Data .....		64
<b>Figure F2.</b>	Run 4 2/24/94 Raw Data .....		66
<b>Figure F3.</b>	Run 5 2/24/94 Raw Data .....		68

## LIST OF SYMBOLS

$a_0$ - $a_6$	Coefficients of Eq. (5)
$b_0$ - $b_3$	Coefficients of Eq. (6)
$C_p$	Specific heat at constant pressure
$d_s$	Distance of one blade space
$d_1$	Staggered passage width
$M$	Mach number
$P$	Pressure
$P_T$	Stagnation (total) pressure
$P_1$	Probe pressure (center tube)
$P_2$	Probe pressure (side hole-facing down)
$P_3$	Probe pressure (side hole-facing up)
$P_{23}$	Average of $P_2$ and $P_3$
$T_T$	Stagnation temperature
$V$	Velocity
$V_T$	Limiting velocity
$X$	Dimensionless velocity
$B$	Defined by Eq. (3)
$\beta_i$	Flow angle
$\gamma$	Ratio of Specific Heats
$\Gamma$	Defined by Eq. (4)
$\theta$	Flow angle to the probe axis ( and to inlet flow direction)
$\phi$	Pitch angle
$\Phi$	Pitch angle at $X_i$ =constant

$\overline{\omega}$	Mass-averaged loss coefficient
$\omega_{\text{mixed}}$	Mixed-out loss coefficient defined in Appendix E, Eq. (13)

## ACKNOWLEDGEMENTS

I would like to take this opportunity to thank those people who have made my time at NPS such a rewarding experience. Professor Raymond Shreeve has kept me centered on my objectives and taught me not only the principles of turbomachinery, but also the proper method of engineering research. His patience and attention to detail was a positive influence on me. Professor Garth Hobson's enthusiasm and energy provided an outstanding environment for work and learning at the Turbopropulsion Lab. I am grateful to Rick Still and Thad Best for their skill at operating the transonic cascade wind tunnel and free-jet. I would like to thank John Moulton for crafting such an excellent probe tip for use in the transonic cascade traverse system. I am also grateful to Don Harvey and Pat Hickey for their skilled advice in the design of the probe calibration apparatus. Finally, I thank my wife Rachel, whose love, support, and constant encouragement has kept me focused on my goals and the light at the end of this tunnel.



## I. INTRODUCTION

The requirement to achieve higher compressor ratios in the fan stages of military and civilian engines has led to increasing supersonic relative inlet Mach numbers. The higher Mach numbers lead to stronger shock waves forming in the rotor passages near the blade leading edge. These strong shocks interact with the turbulent boundary layer on the suction side of each blade to produce the flow field depicted in Figure 1.

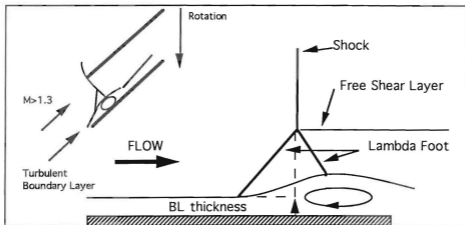
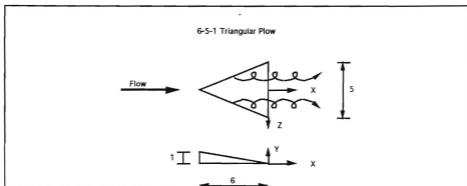


Figure 1. Shock-Boundary Layer Interaction

The shock-boundary layer interaction is characterized by the lambda foot and a local region of reversed flow. The strong shock-boundary layer interaction adversely effects the total pressure ratio and flow turning angle of the compressor blade row. A concept for alleviating the shock-induced boundary layer separation is the use of low-profile vortex generators affixed to the suction surface of the rotor blading, some distance ahead of where the shock impinges.

Vortex generator devices alleviate the shock interaction by energizing the low momentum region of the boundary layer with relative near-freestream flow via streamwise vortices. The vortex generators reduce the relative total pressure loss in the rotor by reducing the size of the local separation and also improve the flow turning angle toward that required by the design. In the present study, 6-5-1 "Triangular Plow Vortex Generators", depicted in Figure 2 and described by McCormick [Ref. 1] and United Technologies Research Center [Ref. 2], were to be used in a model transonic Fan-Blade cascade to quantify their effect on the total pressure losses and flow turning angle and thereby assess the potential benefits of this technique.



**Figure 2.** Low-Profile Vortex Generator

The model cascade apparatus was first assembled and operated by Collins [Ref. 3]. First successful static pressure measurements were made by Golden [Ref. 4] and impact probe traverse measurements by Myre [Ref. 5]. Tapp [Ref. 6] showed that repeatable periodic conditions could be achieved at the design flow angle using wall bleed. In the present study, a three-port traversing pneumatic probe was designed, calibrated, and used to measure dimensionless velocity and

flow angle over the outlet of a blade passage. These values were used to calculate a fully-mixed-out condition, and hence the total pressure loss and flow turning angle. A follow-on study will apply the techniques reported here to assess the effects of vortex generators. In the present document, Chapter II describes the design and calibration of the three-port probe and the transonic fan-blade cascade model. Chapter III describes the experimental program and test results. Chapter IV includes the conclusions and recommendations for further work.

## II. EXPERIMENTAL DEVELOPMENTS

### A. PROBE DESIGN

To measure Mach number and flow angle behind the model fan-blade passage required a probe that was sensitive to only Mach number and pitch angle, since the yaw angle was zero at mid-span. It was desirable (though not necessary) that the arrangement of sensors would result in two pressure coefficients such that one was insensitive to changes in pitch angle at constant Mach number and the other insensitive to changes in Mach number at constant pitch angle. AGARD-AG-207 [Ref. 7] reported probe designs that had such characteristics, which guided the present design shown in Figure 3.

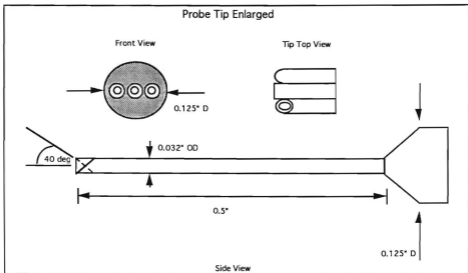


Figure 3. Probe Tip Enlarged

Additionally, the probe was required to measure velocities in a shear layer as it traversed through the fan-blade wake, which required that the ports all lie in the same plane. Myre [Ref. 5] developed a traversing impact probe system for use in the present experiment with the ability to accommodate different probe tips. The present probe was designed to fit the existing probe holder and traverse system for use with the current data acquisition system hardware and software reported by Myre [Ref. 5]. A three-port pneumatic probe was chosen using 0.032" OD stainless steel tubing. The center port was cut normal to the tunnel axis with the outer two ports shaved to an angle of approximately forty degrees in opposite directions.

## **B. PROBE CALIBRATION**

The probe calibration was carried out in the Turbopropulsion Laboratory's free-jet calibration apparatus which is shown in Figure 4. The probe holder assembly is described by Myre [Ref. 5] and depicted in Figure 5. The nozzle of the free-jet was 4.25 inches in diameter and was fed by an Allis-Chalmers compressor delivering air at a pressure of up to three atmospheres. The Mach number range of the free-jet, which exhausted to atmosphere, was from 0 to 0.9. The probe holder was attached to an apparatus mounted to the free-jet nozzle which allowed the operator to accurately set and vary the pitch angle of the probe, as required for the calibration. A Prandtl probe was installed 0.5 inches from the jet centerline to provide redundancy in the measurement of Mach number.

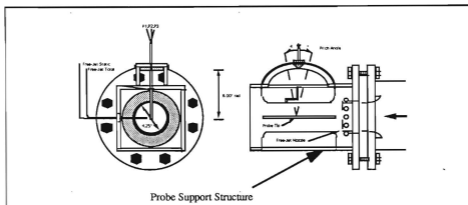


Figure 4. Free-Jet Calibration Apparatus

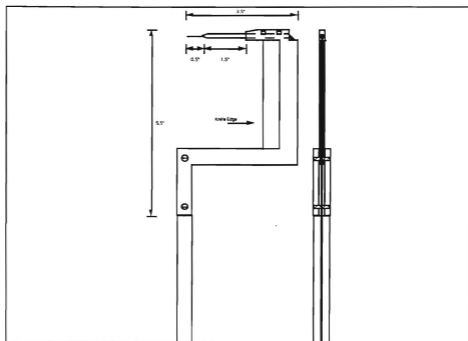


Figure 5. Probe Holder Assembly

## 1. Data Acquisition System

The pressure measurements of the probe (3), free-jet static pressure (atmospheric), and free-jet total pressure were acquired using a +/- 50 psid Scanivalve transducer controlled by a Hewlett-Packard 9000-300 series computer. The HP 9000 computer sent commands via a HG-78K Scanivalve controller developed by Geopfarth [Ref. 8] to the Scanivalve. It in turn sent the measured voltage of the transducer to a HP 3456A digital voltmeter, which was read by the computer. The voltages were recorded and converted to psia in an HP BASIC data acquisition program, "CAL\_ACQ", listed in Appendix A. Golden [Ref. 4] describes in detail the use of the data acquisition system.

## 2. Program of Measurements

The impact probe and probe assembly were removed from the transonic cascade and the new three-port probe design was installed. The new probe and probe holder assembly were mounted in the free-jet calibration apparatus. The probe was leveled in its mount, then securely fastened in place. The probe tip was located at the center of the free-jet, which has been shown to have a uniform velocity profile by Neuhoﬀ [Ref. 9]. The free-jet static and total pressures were used to calculate the jet Mach number and limiting velocity using isentropic gas relations with the ratio of specific heats equal to 1.4. The relation between total (stagnation) pressure, static pressure, and dimensionless velocity is

$$\frac{P}{P_T} = \left(1 - X^2\right)^{\frac{\gamma}{\gamma-1}} \quad (1)$$

where

$$X = \frac{V}{\sqrt{2C_p T_T}}$$

The Mach number was held stable while 12 pitch angles were set in turn and pressure data were recorded. The Mach number was varied in steps of 0.1 from  $M = 0.2$  to  $0.9$ , giving a total of 96 calibration data points. In the calculation of dimensionless velocity the center port pressure measurement was taken to be total pressure since it was always in the center of the flow and always read slightly higher than the Prandtl probe total pressure. The static pressure was taken to be atmospheric, which was consistent with the Prandtl probe measurements. The raw data from the calibration are listed in Table B1 and Table B2 of Appendix B.

### 3. Probe Characteristics

The derivation of the probe pressure coefficients followed the work of Neuhoﬀ [Ref. 9]. If  $P_1$  is the pressure at the center port and  $P_2$  and  $P_3$  are the pressures of the two side ports, we define the average of  $P_2$  and  $P_3$  as  $P_{23}$ , where

$$P_{23} = \frac{P_2 + P_3}{2} \quad (2)$$

and the two pressure coefficients used to represent the calibration of the probe in terms of Mach number and pitch angle are

$$\text{Beta} = B = \frac{P_1 - P_{23}}{P_1} \quad (3)$$

and

$$\text{Gamma} = \Gamma = \frac{P_2 - P_3}{P_1 - P_{23}} \quad (4)$$

The measured characteristics of the probe in terms of Beta and Gamma are shown in Figures 6 and 7 respectively. The Mach-sensitive coefficient Beta

was found to be relatively insensitive to changes in pitch angle over the entire Mach range. The pitch sensitive coefficient Gamma was found to be relatively insensitive to changes in Mach number over the range of pitch angles.

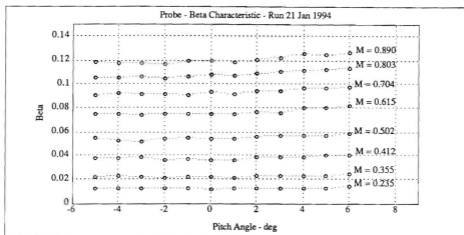


Figure 6. Beta Characteristic

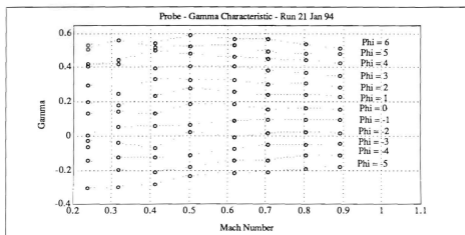


Figure 7. Gamma Characteristic

The insensitivity of Beta to pitch angle allowed the Mach number and dimensionless velocity, X, to be approximated by a polynomial in terms of Beta only. The polynomial for X as a function of Beta was derived utilizing the least-squares method, using an average value of Beta over the range of pitch angle. The program MATLAB was used to determine this polynomial and a choice of a sixth-order polynomial was found to give the least error in X over the calibration range. The polynomial is shown as Equation 5, with the values of the coefficients listed below. The sixth-order polynomial is shown and plotted vs. the actual data points in Appendix C.

$$\begin{aligned}
X &= a_6 B^6 + a_5 B^5 + a_4 B^4 + a_3 B^3 + a_2 B^2 + a_1 B + a_0 \\
a_6 &= -1733913.202 \\
a_5 &= +679216.632 \\
a_4 &= -104416.881 \\
a_3 &= +8119.488 \\
a_2 &= -344.912 \\
a_1 &= +10.120 \\
a_0 &= +0.018
\end{aligned} \tag{5}$$

A third-order polynomial for pitch angle was derived in terms of Gamma at each average dimensionless velocity using the least-squares method and the MATLAB software. The polynomial has the form of Equation 6 with the coefficients summarized in Table I. The third-order polynomials of pitch angle in terms of Gamma are plotted vs. the actual data points in Appendix C.

$$\Phi_i = b_3 \Gamma^3 + b_2 \Gamma^2 + b_1 \Gamma + b_0 \tag{6}$$

where

$$X_i = \text{constant}$$

**TABLE 1. PROBE CALIBRATION COEFFICIENTS**

	$X_i$	$b_3$	$b_2$	$b_1$	$b_0$
$\Phi_1$	0.1047	-0.815	3.584	12.251	-1.841
$\Phi_2$	0.1397	0.156	0.412	12.112	-1.548
$\Phi_3$	0.1812	19.817	-5.526	9.996	-1.461
$\Phi_4$	0.2192	13.149	-3.288	11.104	-1.973
$\Phi_5$	0.2650	15.897	-5.546	12.155	-2.072
$\Phi_6$	0.3002	3.438	0.520	13.270	-2.268
$\Phi_7$	0.3378	11.242	-2.607	13.736	-2.349
$\Phi_8$	0.3698	11.968	-3.634	14.607	-2.347

#### **4. Application of the Calibration**

The method of application of the calibration was first to take the measured probe pressures and determine the coefficients Beta and Gamma. From the Beta coefficient, the dimensionless velocity could be determined immediately using the sixth-order polynomial. With the dimensionless velocity known, the third-order polynomials of pitch angle in terms of Gamma could be calculated for the curves associated with the values of the dimensionless velocity above and below the calculated dimensionless velocity. An interpolation scheme given by Nakamura [Ref. 10] was then used to interpolate for the pitch angle at that known velocity and value of Gamma. The results of applying the calibration method to the actual data is given in Appendix C. Over the entire range of the calibration the uncertainty in dimensionless velocity was found to be +/- two percent with a confidence of 70 percent. The pitch angle uncertainty was found

to be  $\pm 0.2$  degrees with a confidence of 76 percent. Above a dimensionless velocity value of 0.18, the confidence level increased due to the improved resolution of the data acquisition system at the higher velocities. Above this velocity, where most of the cascade measurements were to be taken, the confidence in determining dimensionless velocity and pitch angle accurately rose to 73 percent and 96 percent respectively. A Kline and McClintock uncertainty analysis [Ref. 11] was performed and at the lower velocities,  $X < 0.18$ , the uncertainty in Beta and Gamma was much higher than at the higher velocities. This explains why the calibration scheme is more accurate at the higher velocities and why the Gamma characteristic behaves poorly at lower velocities. The calibration application program, written in Hewlett-Packard Basic is listed in the data reduction program "NEW\_READ\_ZOC1", in Appendix D.

## **C. TRANSONIC CASCADE MODEL AND DATA ACQUISITION**

### **1. Transonic Cascade Model**

The transonic cascade model attempts to simulate the relative flow at  $M=1.4$  on a stream surface through a Navy developmental transonic fan. The current model has been shown by Golden [Ref. 4] to be closely two dimensional with the placement of the shock structure set manually using an in-line shadowgraph while adjusting back pressure and bleed valves. The vertically-traversing probe assembly designed by Myre [Ref. 5] was used with the new probe design. Myre also describes the use of the traversing system [Ref. 5]. The wind tunnel facility is shown schematically in Figure 8. The transonic cascade model test section is shown in Figure 9. The model simulation is of the flow through two passages of the transonic blading geometry which is shown in Figure 10. In the cascade simulation, the design pressure ratio and shock

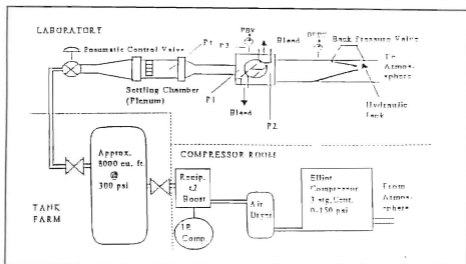


Figure 8. Wind Tunnel Facility

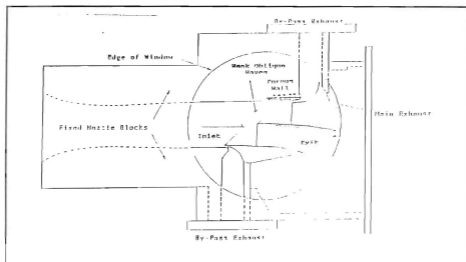


Figure 9. Transonic Cascade Model Test Section

structure at the design incidence were set using the "Back-Pressure Valve (BPV)". A "Back-Pressure Bleed Valve (BPBV)" was used for fine adjustments in setting the proper shock structure (Figure 8).

## **2. Data Acquisition System**

The data acquisition system utilized in the present study was used previously by Tapp [Ref. 6]. One +/- 50 psid ZOC-14 enclosure was used to record the three pressures of the traversing probe. Plenum and wall reference pressures were also recorded. The data acquisition program "NEW\_SCAN\_ZOC" [Ref. 5] was modified slightly to allow the probe-traverse mechanism to increment in smaller steps through the wake, in order to improve the spatial resolution. To change the increment step size required a change in only a single line of code. The initial starting point of the probe-traverse assembly was also changed by a single entry.

The data reduction program "READ\_ZOC2" [Ref. 5] was modified for use in the current study and renamed "NEW\_READ\_ZOC1". The principal change was the application of the routine to return dimensionless velocity and flow angle from the three pressure measurements. The calculation of the fully-mixed-out condition was also calculated in the program. The program is listed in Appendix D and the calculation of the fully-mixed-out condition is summarized in Appendix E. A complete derivation of the method for calculating the fully-mixed-out dimensionless velocity, flow angle, and total pressure is contained in Reference 12.

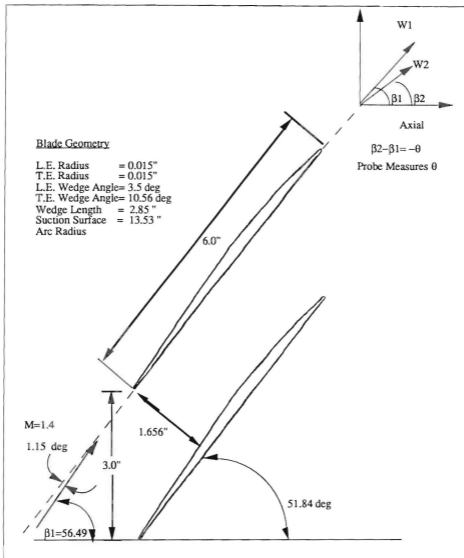


Figure 10. Cascade Blading Geometry

### III. EXPERIMENTAL PROGRAM, RESULTS AND DISCUSSION

#### A. EXPERIMENTAL PROGRAM

The experimental program consisted of a series of initial runs with equal-increment probe traverses through the center blade wake. These tests were used to refine the operation of the pressure valves in setting the shock structure, to become familiar with the data acquisition procedures, and to verify the revised coding of the data reduction program "NEW\_READ\_ZOC1". Repeatability tests were then conducted to verify that the impact probe measurements compared with previous results reported by Myre [Ref. 5] and Tapp [Ref. 6]. Once these tests were completed the number of data points in the blade wake was increased to provide better resolution through the wake. These tests were used to examine probe-derived static pressure and angle distributions through the wake. Finally, five tests were conducted to provide baseline data and to establish the fully-mixed-out condition for use in studies to assess the effect of vortex generating devices. In all the tests, the shocks in the upper and lower passages were repeatedly set to the expected on-design position, using the following procedure:

- 1. The tunnel was allowed to become steady at a plenum pressure of 33 psig.
- 2. While carefully monitoring the shadowgraph, the BPV was closed by four smooth movements of the hydraulic jack handle.

- 3. A fifth movement of the jack handle (done smoothly) was stopped just as the lower passage shock was in position at a mark on the tunnel side plate (visible in the shadowgraph).
- 4. The BPBV was closed until the upper passage shock was in the corresponding position. Its position was monitored visually throughout the data acquisition during the probe traverse.

## B. REPEATABILITY TESTS

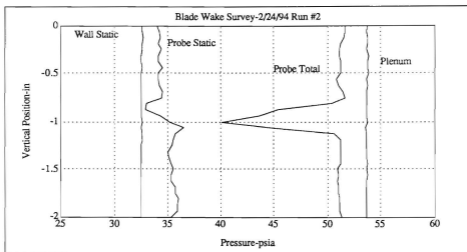
These tests were run to compare the mass-averaged loss coefficient results obtained with the new probe and those obtained by Myre [Ref. 5] and Tapp [Ref. 6], using an equal-increment traverse procedure, across a distance of two inches. The probe tip was approximately 1 1/8 inches downstream of the trailing edge of the middle blade with the probe starting its traverse 1.0 inch above the level of the blade trailing edge. Figures 11 and 12 show the blade-wake pressures vs. vertical position during the traverse. Table 2 summarizes the results of tests in which tunnel supply conditions were held reasonably constant.

TABLE 2. REPEATABILITY TESTS: 2/24/94 RUN 2 AND RUN 4

Run #	Patm (psia)	P2/P1	T <sub>T</sub> (R)	$\bar{w}$
2	14.72	2.11	514.5	0.0842
4	14.715	2.09	513.0	0.0847

The raw pressure data for the complete test program are listed in Appendix F. The mass-averaged losses compared well ( to within three percent) with previous results [Ref. 5 & 6] with similar tunnel conditions. The data confirmed that the

probe, data acquisition system, and data reduction process were operating properly.



**Figure 11.** Blade Wake Survey: 2/24/94 Run 2

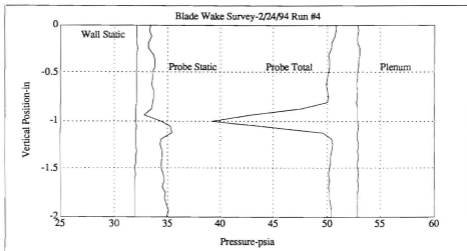


**Figure 12.** Blade Wake Survey: 2/24/94 Run 4

Probe-derived static pressure profiles are shown in Figures 11 and 12. It is seen that the static pressure on the suction side of the blade was lower than that on the pressure side, implying a higher velocity in that portion of the upper passage. A change in static pressure through the wake can clearly be seen. Both runs show a reasonably periodic condition in the cascade model based only on the measured total pressure.

### C. TURNING ANGLE DISTRIBUTION

Figure 13 shows the distribution of the flow angle derived from probe measurements in three similar tests.

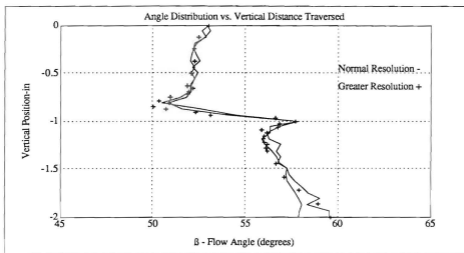


**Figure 13.** Angle Distribution Comparison

Figure 13 contains data from Runs 2, 4, and 5 of 2/24/94. As presented previously, Runs 2 and 4 were equal-increment surveys for a two inch traverse. Run 5 was a survey which stepped 0.03125 inches per increment through 22 points just prior to, and through the blade wake, providing better spatial

resolution. The start and end points remained the same for all three runs. The data are seen to be similar for all runs. The angle distribution is characterized by increased values of outlet flow angle ( $\beta_2$ ) from the upper portion of the lower passage (less turning). The value of  $\beta_2$  from the upper passage approaches that of the design value of 50 degrees. The flow angle behaves similarly to the static pressure through the turbulent blade wake. Without further measurements, the differences in flow angle and dimensionless velocity cannot be explained definitively. The higher turning angle in the upper passage and lower turning angle in the lower passage is most probably the result of the significant differences in the wakes of the center and lower blades. The center blade is a true blade wake, the lower blade wake is a mixing layer, with entrainment from the test section cavity. In viewing the probe distributions, it should be remembered that the traverse was not parallel to the blade trailing edges so that the lower part of the traverse is further downstream of the blading than is the upper part. The data do show that the angle distributions through the passages were repeatable.

#### **D. PROBE STATIC PRESSURE DISTRIBUTION**

Figure 14 shows a comparison of probe-derived static pressure for the same tests as in Figure 13. The static pressure distributions all have the same form, and were reasonably repeatable. The improved resolution blade-wake surveys clearly show a steep decline in static pressure as the probe entered the blade wake, then a sharp rise through the wake. The static pressure rises slightly again on the pressure side of the blade wake, then stabilizes at a value above that of the upper passage.

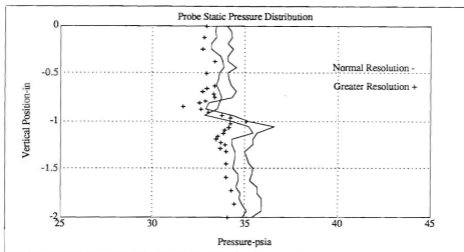


Figure 14. Probe Static Pressure Distribution

#### E. MODEL BASELINE MEASUREMENTS

The model baseline measurements were made using a survey distance of 1.656 inches (equal to the staggered-pass width, Figure 10) with the probe starting position located 0.75 inches above the level of the middle blade trailing edge. ZOC 1 was used for the probe surveys with the measured pressures and their associated ports listed in Table 3. Table 4 lists the probe positions relative to the starting point with point 1 being the beginning of the traverse above the middle blade. Five runs were made to determine the flow profiles and the baseline loss coefficient using the fully-mixed-out conditions calculated as shown in Appendix E. Table 5 lists the tunnel conditions for the five runs and Table 6 lists the results of the fully-mixed-out calculations. Figures 15 through 19 show the blade wake survey results output by the data reduction program "NEW\_READ\_ZOC1".

**TABLE 3. MEASURED PRESSURES AND PORTS ASSIGNED**

Measured Pressure psia	Port Assigned
Atmospheric	1
P1	32
P2	24
P3	25
Upstream Static	29
Downstream Static	30
Plenum	31

**TABLE 4. PROBE TRAVERSE POSITON**

Point	Relative Position-in	Point	Relative Position-in	Point	Relative Position-in
1	0	12	0.50	23	0.84375
2	0.0625	13	0.53125	24	0.875
3	0.125	14	0.5625	25	0.90625
4	0.1875	15	0.59375	26	0.9375
5	0.25	16	0.625	27	0.96875
6	0.3125	17	0.65625	28	1.00
7	0.34375	18	0.6875	29	1.13125
8	0.375	19	0.71875	30	1.2625
9	0.40625	20	0.75	31	1.39375
10	0.4375	21	0.78125	32	1.525
11	0.46875	22	0.8125	33	1.65625

TABLE 5. BASELINE TUNNEL CONDITIONS

Run #	Upstream Static-psia	P2/P1	T <sub>T</sub> (R)	Plenum- psia	Mass Flux Integral
1	15.279	2.09	518.7	48.45	0.9143
2	15.128	2.08	519.7	47.94	0.9140
3	15.379	2.08	518.2	48.76	0.9196
4	15.043	2.07	518.2	47.75	0.9218
5	15.047	2.09	517.7	47.65	0.9227

TABLE 6. BASELINE FULLY-MIXED-OUT CONDITIONS

Run #	X <sub>3</sub>	Pt <sub>3</sub> - psia	$\beta_3$ -deg	$\sigma_{mixed}$
1	0.3115	40.73	55.14	0.2328
2	0.3118	40.31	55.15	0.2327
3	0.3100	40.58	54.73	0.2450
4	0.3159	39.76	55.05	0.2443
5	0.3143	39.73	54.92	0.2432
AVERAGE	0.3127	40.22	55.00	0.2396

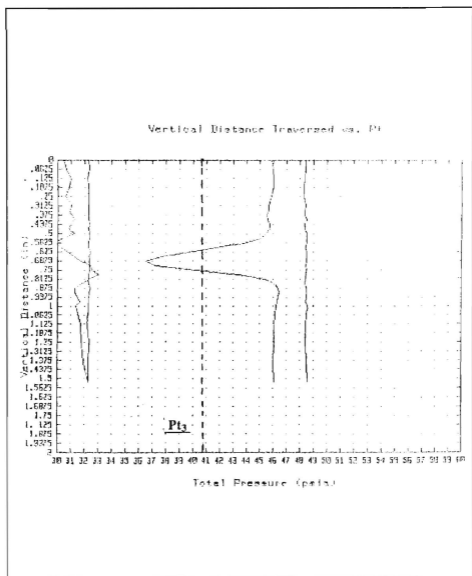


Figure 15. Baseline Blade Wake Survey: Run 1

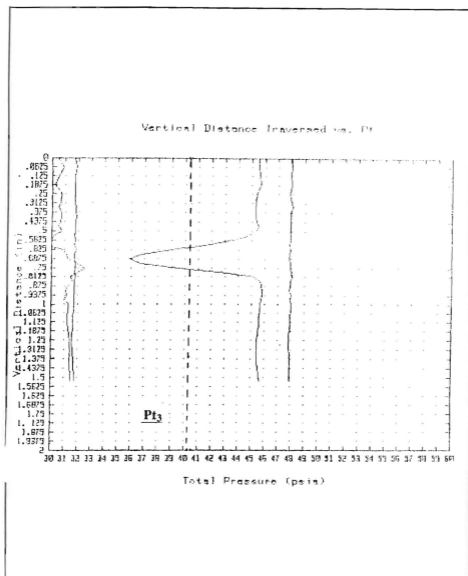


Figure 16. Baseline Blade Wake Survey: Run 2

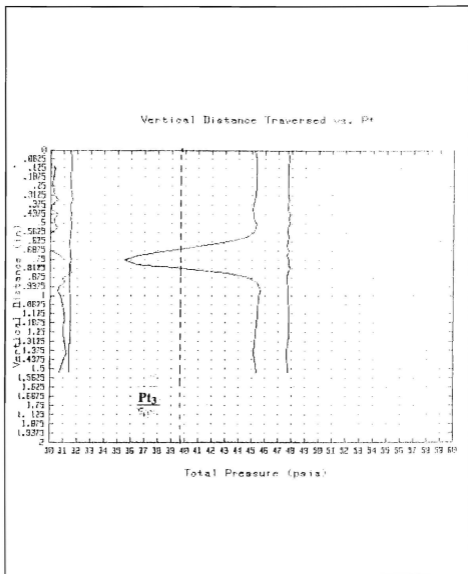


Figure 17. Baseline Blade Wake Survey: Run 3

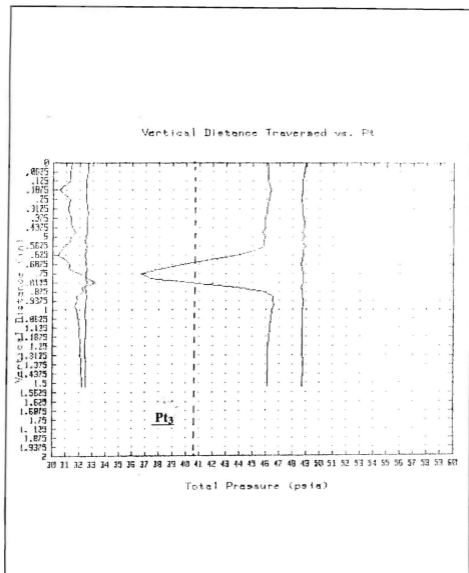


Figure 18. Baseline Blade Wake Survey: Run 4

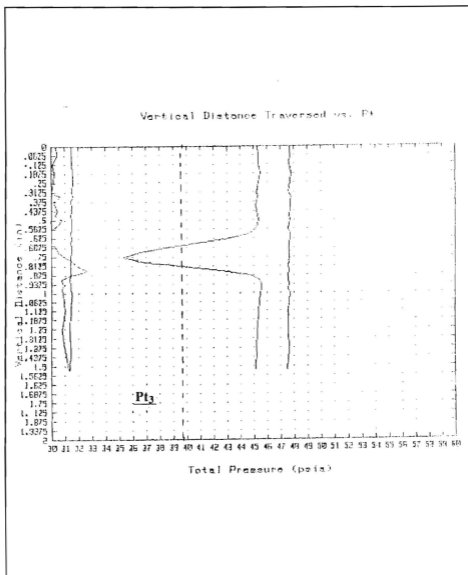


Figure 19. Baseline Blade Wake Survey: Run 5

In all cases, the calculated fully-mixed-out total pressure ( $P_{t3}$ ) was repeatable and qualitatively showed a low but not unreasonable value when compared to probe-measured total pressure distribution, which was reasonably periodic. The probe-derived static pressure distributions were also repeatable, and followed the trends of the previously discussed results. The calculated fully-mixed-out loss coefficient was more than twice the mass-averaged loss coefficient as presented in Table 2. The fully-mixed-out calculation subprogram in "NEW\_READ\_ZOC1" was verified by programming a known test case used by Armstrong [Ref. 12]. It is noted that the test case was at low Mach number, rather than the high subsonic range of the present measurements. However, it is also noted that Armstrong also reported that much higher values were obtained for the fully-mixed-out loss coefficient than for the mass-averaged loss coefficient, when reducing cascade-flow survey data.

#### IV. CONCLUSIONS AND RECOMMENDATIONS

In the present study, the velocity and flow angle distributions, and the fully-mixed-out losses due to the shock-boundary layer interaction in the transonic fan-blade cascade model, were measured at the design incidence angle. The measured flow field and flow losses provide baseline values for planned measurements with low-profile vortex generator devices installed. The fully-mixed-out loss values were more than twice the mass-averaged loss values reported by Myre [Ref. 5] and Tapp [Ref. 6] and repeated in the present study. The measurements of pressure and flow angle distributions were repeatable. The three-port probe, designed for the present study, gave excellent results in measurements of static pressure, dimensionless velocity and flow angle, at velocities greater than  $M = 0.4$ .

The following specific conclusions were drawn:

- Shock placement using the Back Pressure Valve (BPV), Back Pressure Bleed Valve (BPBV), Porous Bleed Valve (PBV), and in-line shadowgraph system was quick, and gave repeatable results.
- The calculated fully-mixed-out flow losses were significantly higher than mass-averaged results. This may have been due to the probe not traversing parallel to the trailing edge, but a more detailed analysis of how this would effect the calculation needs to be made.
- The probe-derived static pressure in the flow from the suction side of the center blade was lower than that from the pressure side, indicating a higher velocity in the upper passage.

- Angle distributions obtained in the surveys were repeatable and showed less flow turning from the pressure side of the middle blade than from the suction side.
- The probe in its present location, traversing normal to inlet velocity, could not determine the degree of periodicity in the two-passage fan-blade model.
- The probe design had excellent characteristics at medium to high Mach numbers and had the ability to measure accurately in the wake shear layers. Measurements of static pressure and flow angle through the blade wake were consistent with previous experience at lower Mach numbers [Ref. 13].

The following recommendations are made concerning the present pilot and follow-on research program:

- Use the same probe design but increase the range of the angle calibration from -6 degrees to +12 degrees.
- Design and build an apparatus to calibrate the probe in the probe holder while still attached to the motor-controller assembly and utilizing the ZOC system for data acquisition.
- Make more measurements with the current system and validate the calculation of the fully-mixed-out loss .
- Install the 6-5-1 Triangular Plow Vortex Generator Devices and compare the loss measurements and the flow field to the baseline results.

- Once these pilot experiments are complete, proceed to a larger apparatus in which Mach number and cascade geometry can be varied. In the larger apparatus, design the traverse to be parallel to the blade trailing edge.
- The larger apparatus should incorporate three blades to improve the ability to simulate periodicity.

## APPENDIX A. PROGRAM "CAL\_ACQ"

```

10  OPEN UNIT1      USE APP
20  DIMENSION  C(100,10)
30  C = 0.0
40  CLOSE UNIT1
50  OPEN UNIT2
60  C = 0.0
70  C = 0.0
80  C = 0.0
90  C = 0.0
100 C = 0.0
110 C = 0.0
120 C = 0.0
130 C = 0.0
140 C = 0.0
150 C = 0.0
160 C = 0.0
170 C = 0.0
180 C = 0.0
190 C = 0.0
200 C = 0.0
210 C = 0.0
220 C = 0.0
230 C = 0.0
240 C = 0.0
250 C = 0.0
260 C = 0.0
270 C = 0.0
280 C = 0.0
290 C = 0.0
300 C = 0.0
310 C = 0.0
320 C = 0.0
330 C = 0.0
340 C = 0.0
350 C = 0.0
360 C = 0.0
370 C = 0.0
380 C = 0.0
390 C = 0.0
400 C = 0.0
410 C = 0.0
420 C = 0.0
430 C = 0.0
440 C = 0.0
450 C = 0.0
460 C = 0.0
470 C = 0.0
480 C = 0.0
490 C = 0.0
500 C = 0.0

```

Figure A1. Program "CAL\_ACQ"



**Figure A1.** (cont) Program "CAL ACO"



# APPENDIX B. PROBE CALIBRATION RAW DATA

TABLE B1. PROBE CALIBRATION RAW DATA X = 0.10 - 0.22

ANGLE (deg)	P1 (psia)	P2 (psia)	P3 (psia)	PSTAT (psia)	P10 (psia)	P2 & P3 avg	X	GAMMA	BETA
-5	15.4089	15.1831	15.2424	14.8421	15.3847	15.21275	0.1030245	-0.30543394	0.0126015
-4	15.4051	15.207	15.2288	14.8217	15.359	15.2139	0.10473862	-0.13493224	0.0124144
-3	15.412	15.2172	15.228	14.8271	15.365	15.2228	0.10484925	-0.05702218	0.01228913
-2	15.413	15.2133	15.2178	14.83	15.3644	15.21545	0.104873	-0.02176644	0.0128171
-1	15.4092	15.2139	15.212	14.8278	15.3684	15.21295	0.10453122	0.00988153	0.0127359
0	15.4059	15.2353	15.2104	14.825	15.3591	15.22285	0.10410681	0.13602841	0.01188131
1	15.4063	15.24	15.2029	14.8277	15.3615	15.22145	0.10428477	0.20070327	0.01194883
2	15.422	15.2527	15.1831	14.8292	15.3692	15.2229	0.1055302	0.29934708	0.01291013
3	15.4132	15.2574	15.174	14.8223	15.3688	15.2157	0.10538908	0.42227848	0.01281369
4	15.4128	15.2509	15.1687	14.8258	15.3484	15.2098	0.10503718	0.40492611	0.01317087
5	15.4177	15.2603	15.1581	14.8252	15.3711	15.2082	0.10498581	0.50499136	0.01313937
6	15.4224	15.2587	15.141	14.8241	15.359	15.19985	0.1080242	0.52886992	0.01443031
-5	15.8937	15.4878	15.592	14.8261	15.8155	15.5398	0.14025233	-0.29499959	0.02225888
-4	15.9032	15.5064	15.5722	14.8272	15.8343	15.5418	0.14078927	-0.19574233	0.02274342
-3	15.8946	15.528	15.5892	14.8289	15.826	15.5488	0.14012025	-0.11907514	0.0217684
-2	15.8884	15.5387	15.5504	14.8363	15.8078	15.54455	0.13922888	-0.03402647	0.02164157
-1	15.9001	15.5428	15.544	14.8282	15.8159	15.5533	0.14051286	0.05363322	0.02181118
0	15.9038	15.5784	15.5248	14.8319	15.8189	15.5525	0.14048959	0.14681781	0.02221482
1	15.8893	15.5801	15.5177	14.8373	15.817	15.5489	0.13921786	0.18331375	0.02145322
2	15.8948	15.5785	15.4889	14.842	15.8168	15.5327	0.13925374	0.25228895	0.02278718
3	15.902	15.6135	15.4581	14.8454	15.8092	15.5363	0.13947239	0.42222039	0.02299711
4	15.9012	15.6104	15.4453	14.8434	15.8202	15.52785	0.13955715	0.4442124	0.02347836
5	15.8893	15.624	15.4178	14.8403	15.8314	15.5209	0.13987836	0.5597177	0.02318541
6	15.9048	15.6245	15.4049	14.8523	15.8731	15.5147	0.13916955	0.56322134	0.02451492
-5	18.7033	18.9884	18.1823	14.8523	18.5731	18.07435	0.18168117	-0.27867247	0.03765424
-4	18.7008	18.0078	18.1383	14.8479	18.5051	18.07195	0.18178352	-0.20472441	0.03784236
-3	18.7146	18.0353	18.1104	14.8482	18.5912	18.07285	0.18238386	-0.11702378	0.03830458
-2	18.688	18.084	18.1058	14.852	18.5889	18.0849	0.18087829	-0.05830857	0.03813974
-1	18.6889	18.0893	18.0517	14.8503	18.5858	18.0705	0.18110581	0.08080207	0.03705457
0	18.6883	18.1223	18.0417	14.8521	18.5806	18.082	0.18098687	0.13293749	0.03833284
1	18.6791	18.1497	18.0074	14.8482	18.5721	18.07855	0.18076623	0.23649448	0.03800814
2	18.6949	18.1893	15.9408	14.8534	18.564	18.05805	0.18122177	0.33995448	0.03814838
3	18.6901	18.181	15.9271	14.853	18.5387	18.0541	0.18102295	0.38937107	0.03810842
4	18.6888	18.201	15.8783	14.8537	18.5511	18.03885	0.18082878	0.48880207	0.03877083
5	18.7041	18.2085	15.885	14.8534	18.5727	18.03895	0.18184127	0.51849298	0.03888102
6	18.7018	18.2124	15.8461	14.8582	18.5701	18.02025	0.18128133	0.54440553	0.04025862
-5	17.8875	18.6005	16.8234	14.8895	17.4869	16.71195	0.21948884	-0.22848308	0.05518011
-4	17.882	18.6495	16.8131	14.8781	17.5308	16.7313	0.21868806	-0.17578167	0.05268505
-3	17.8384	18.6728	16.7724	14.8804	17.5167	16.7226	0.21852902	-0.1089954	0.0518133
-2	17.8674	18.7212	16.8948	14.8852	17.4827	16.708	0.21841922	0.0275172	0.05430341
-1	17.8858	18.742	16.8751	14.8864	17.4886	16.70855	0.22001339	0.06845741	0.05525619
0	17.8847	18.8048	16.8248	14.8898	17.5487	16.7148	0.21923574	0.18949303	0.05577391
1	17.8849	18.8319	16.8579	14.8704	17.5813	16.8949	0.21911454	0.28247423	0.05481115
2	17.8553	18.8562	16.8351	14.8728	17.5308	16.89715	0.21972978	0.32786664	0.05587409
3	17.8904	18.8903	16.4737	14.8707	17.4904	16.882	0.21899539	0.41212971	0.05700267
4	17.8873	18.944	16.424	14.8734	17.5038	16.86425	0.21911539	0.4787854	0.05737886
5	17.8549	18.9102	16.379	14.8718	17.5138	16.8448	0.21870422	0.52578442	0.05722491
6	17.859	18.9328	16.3287	14.875	17.5236	16.82875	0.21871483	0.58887535	0.05828473

TABLE B2. PROBE CALIBRATION RAW DATA X = 0.26 - 0.37

ANGLE (deg)	P1 (psia)	P2 (psia)	P3 (psia)	PSTAT(psia)	PTOT(psia)	P2 & P3 avg	X	GAMMA	BETA
-5	19.2303	17.6324	17.93781	14.9019	19.5151	17.785105	0.26507724	-0.21132788	0.07515197
-4	19.2236	17.6613	17.88121	14.8884	19.0381	17.781255	0.26532258	-0.13860068	0.07522981
-3	19.2013	17.7207	17.82441	14.8889	18.8791	17.772555	0.26475814	-0.07258818	0.07440878
-2	19.2342	17.7631	17.76881	14.8811	18.98	17.788455	0.26554185	-0.00463479	0.07526931
-1	19.2042	17.83	17.68861	14.8231	18.9864	17.764305	0.26489238	0.09124971	0.07497813
0	19.2137	17.9099	17.63551	14.8948	18.9402	17.774705	0.26488897	0.18709197	0.07489492
1	19.221	17.9582	17.5981	14.8448	18.9201	17.789005	0.26527365	0.26606007	0.07554212
2	19.2201	17.9827	17.50731	14.9019	18.919	17.750005	0.26481125	0.33017584	0.07648783
3	19.2022	18.0347	17.43671	14.9005	18.9362	17.735705	0.2643806	0.40776818	0.0763712
4	19.2352	18.0481	17.34021	14.8887	18.9358	17.694055	0.26518222	0.46905258	0.07988919
5	19.233	18.1032	17.26101	14.9018	18.9197	17.697105	0.26515748	0.52885568	0.07988776
6	19.2453	18.115	17.22141	14.9034	18.9288	17.688205	0.26544324	0.58824601	0.08193472
-5	20.7578	18.889	19.0578	14.9191	20.5555	18.8633	0.30008337	-0.20512008	0.0912669
-4	20.7889	18.7415	19.0514	14.9189	20.5097	18.87145	0.3007079	-0.1355446	0.09223432
-3	20.7824	18.849	18.9218	14.9235	20.5139	18.87825	0.3004684	-0.04532113	0.09146232
-2	20.7886	18.9028	18.8654	14.9229	20.5158	18.884	0.30061477	0.01963186	0.09161752
-1	20.7828	18.9754	18.7987	14.9318	20.5023	18.88605	0.30023813	0.09421379	0.09128537
0	20.8028	19.0234	18.7096	14.938	20.5472	18.8865	0.30053062	0.16208166	0.09307882
1	20.7701	19.0977	18.6358	14.9234	20.5548	18.88675	0.30051511	0.24267739	0.09163894
2	20.7821	19.134	18.539	14.9278	20.5648	18.838	0.30055141	0.30486876	0.094079
3	20.7837	19.1791	18.4288	14.941	20.41	18.80385	0.29957054	0.38293747	0.09438828
4	20.7887	19.2317	18.3189	14.9352	20.5188	18.7753	0.30028045	0.45338247	0.09885089
5	20.7878	19.251	18.2592	14.9303	20.5395	18.7551	0.2999869	0.49277709	0.09691445
6	20.7458	19.2889	18.1407	14.9357	20.4787	18.7148	0.29995007	0.56533727	0.09789933
-5	22.8389	20.289	20.7481	15.009	22.4401	20.52355	0.33781229	-0.18608988	0.10521892
-4	22.8201	20.3708	20.6378	14.9969	22.579	20.5043	0.33783964	-0.11052235	0.10540084
-3	22.823	20.4329	20.5426	15.0086	22.6422	20.48715	0.33784505	-0.04504871	0.10621809
-2	22.8085	20.5355	20.4681	15.003	22.5493	20.5008	0.33744501	0.02884815	0.10502252
-1	22.8412	20.6033	20.3666	15.014	22.6714	20.46495	0.33782282	0.09636541	0.1070676
0	22.8388	20.6618	20.257	15.008	22.4862	20.4584	0.33786828	0.16326531	0.10808761
1	22.8355	20.728	20.1675	15.0053	22.8154	20.47055	0.33787852	0.24580729	0.10746535
2	22.8871	20.8813	20.0801	15.005	22.4924	20.4757	0.33840443	0.30954483	0.10847691
3	22.8706	20.9014	19.9547	14.9987	22.8625	20.42805	0.33881829	0.37234273	0.11068714
4	22.9307	20.9408	19.8011	15.0055	22.8417	20.37085	0.33779839	0.44514327	0.11603418
5	22.9279	20.9803	19.7248	15.0059	22.5477	20.34245	0.3378675	0.47794388	0.11378436
6	22.8087	21.0078	19.6188	15.0087	22.517	20.3133	0.3373749	0.5349719	0.11339181
-5	25.185	21.9479	22.461	15.0728	24.9008	22.20445	0.36935398	-0.17214944	0.11834624
-4	25.1712	22.0485	22.3655	15.0751	24.8853	22.207	0.36912206	-0.10894285	0.11778157
-3	25.2068	22.1735	22.2919	15.0745	24.8858	22.2327	0.36960872	-0.03980802	0.1179915
-2	25.1828	22.2658	22.2165	15.0789	25.0103	22.24115	0.36923615	0.0167593	0.11681187
-1	25.2425	22.3807	22.0764	15.0788	24.9345	22.22855	0.37002847	0.10068385	0.11939882
0	25.2558	22.4609	21.9728	15.0715	24.994	22.21675	0.37005558	0.18174605	0.11952943
1	25.2548	22.5048	21.8043	15.0724	24.9458	22.2571	0.37028925	0.23578811	0.11871212
2	25.2359	22.6294	21.7488	15.0771	24.87	22.189	0.36989508	0.28936465	0.12063219
3	25.2277	22.8876	21.5981	15.0747	25.0210	22.14265	0.36887942	0.35317763	0.12224027
4	25.2882	22.8057	21.4402	15.0883	25.0401	22.12285	0.37052159	0.42890838	0.12554745
5	25.2022	22.8202	21.3184	15.0737	24.9398	22.0833	0.3695842	0.47884938	0.12435026
6	25.278	22.8017	21.2615	15.0831	24.7932	22.0818	0.37033101	0.51346106	0.12830776

## APPENDIX C. APPLICATION OF THE CALIBRATION

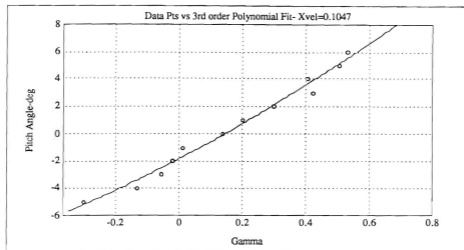


Figure C1. Pitch Angle vs. Gamma X = 0.1047

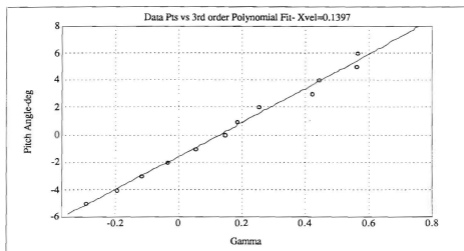


Figure C2. Pitch Angle vs. Gamma X = 0.1397

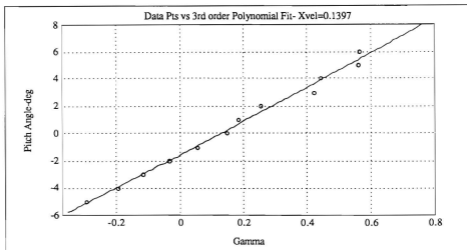


Figure C3. Pitch Angle vs. Gamma X = 0.1812

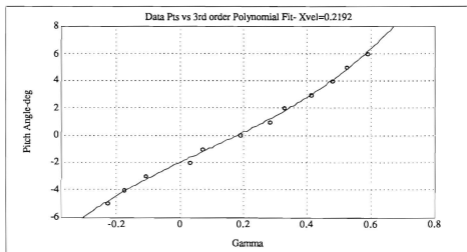


Figure C4. Pitch Angle vs. Gamma X = 0.2192

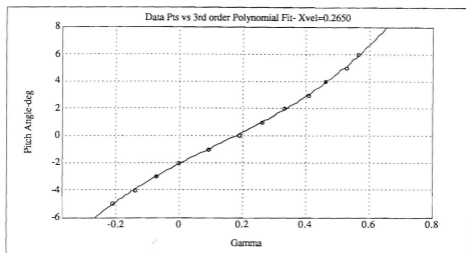


Figure C5. Pitch Angle vs. Gamma X = 0.2650

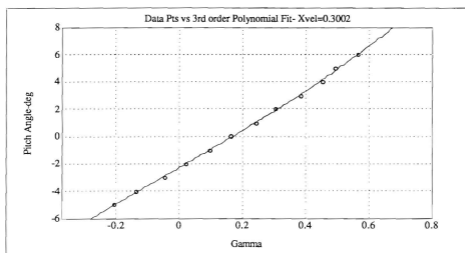
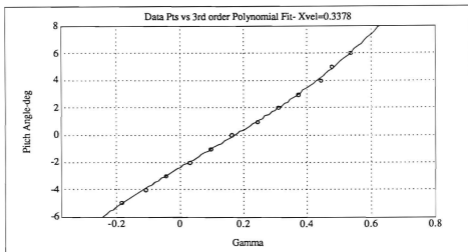
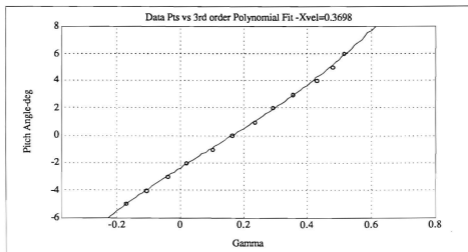


Figure C6. Pitch Angle vs. Gamma X = 0.3002



**Figure C7.** Pitch Angle vs. Gamma  $X = 0.3378$



**Figure C8.** Pitch Angle vs. Gamma  $X = 0.3698$

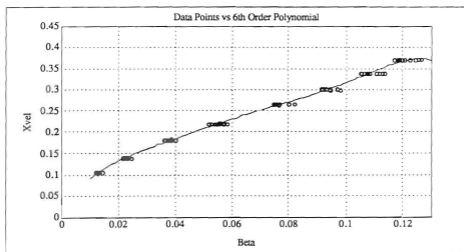


Figure C9. X vs. Beta

TABLE C1. CALIBRATION METHOD RESULTS X = 0.10 - 0.22

ANGLE (deg)	ACTUAL X	CALIBRATED X	CALIBRATED ANGLE	Angle Difference	X % Difference
-5	0.10302443	0.10457949	-5.271	0.271	1.50940746
-4	0.10473655	0.10371192	-3.4375	0.5625	0.97829573
-3	0.10484919	0.10314849	-2.529	0.471	1.62203994
-2	0.10467293	0.10555298	-2.103	0.103	0.84075906
-1	0.10453115	0.10518767	-1.716	0.716	0.62805825
0	0.10450603	0.10124488	-0.109	0.109	3.12053738
1	0.1042947	0.10179391	0.759	0.241	2.39780855
2	0.10553013	0.10596948	2.15	0.15	0.41632236
3	0.10538899	0.10553766	3.93	0.93	0.14107116
4	0.10503711	0.10712581	3.678	0.322	1.98853771
5	0.10499554	0.10698696	5.167	0.167	1.89867253
6	0.10602413	0.11249207	5.517	0.483	6.10044264
-5	0.14025224	0.13980665	-5.09	0.09	0.31770656
-4	0.14079258	0.14122875	-3.91	0.09	0.30979645
-3	0.14012016	0.13829886	-3.01	0.01	1.29999554
-2	0.13922859	0.13791107	-1.988	0.012	0.94630291
-1	0.14051257	0.13841175	-0.919	0.081	1.49511339
0	0.14049581	0.13965073	0.2365	0.2365	0.60149886
1	0.13921777	0.13724023	0.6768	0.3232	1.42046589
2	0.13925365	0.13925365	1.5324	0.4676	2.5998E-06
3	0.1394723	0.1419776	3.647	0.647	1.7962704
4	0.13955706	0.14338869	3.902	0.098	2.74428123
5	0.1388783	0.1443133	5.265	0.265	3.9134965
6	0.13916946	0.14635418	5.55	0.45	5.16257237
-5	0.18166106	0.18007618	-5.124	0.124	0.87243932
-4	0.18176341	0.1800474	-3.92	0.08	0.94408982
-3	0.18238375	0.18186869	-2.749	0.251	0.26338434
-2	0.18097817	0.17639308	-2.231	0.231	2.53350638
-1	0.1811067	0.17862118	-0.8679	0.1321	1.37240608
0	0.18098676	0.1768594	-0.1508	0.1508	2.28047625
1	0.18076512	0.17606679	0.9432	0.0568	2.5996715
2	0.18122165	0.18126723	2.077	0.077	0.02514951
3	0.18102283	0.18117063	2.913	0.087	0.08164354
4	0.18082666	0.18277423	4.608	0.608	1.07703754
5	0.18164116	0.18568528	4.997	0.003	2.22643459
6	0.18128121	0.18634556	5.535	0.465	2.79364135
-5	0.2194901	0.22083929	-4.858	0.142	0.61469162
-4	0.21869114	0.21533631	-4.038	0.038	1.53405034
-3	0.21852929	0.21334476	-3.145	0.145	2.37246331
-2	0.21941948	0.2189379	-1.666	0.334	0.21948013
-1	0.22001366	0.22098927	-1.215	0.215	0.44343307
0	0.219258	0.21775675	0.1151	0.1151	0.68469612
1	0.2191148	0.22028799	1.2	0.2	0.53542175
2	0.21973005	0.22241454	1.789	0.211	1.22127576
3	0.21999585	0.22488684	3.007	0.007	2.22331157
4	0.21911565	0.22438852	4.066	0.066	2.40643095
5	0.21870449	0.22530943	4.899	0.101	3.0200314
6	0.21867328	0.22766856	6.191	0.191	4.11356991

TABLE C2.

## CALIBRATION METHOD RESULTS

X = 0.26 - 0.37

ANGLE (deg)	ACTUAL X	CALIBRATED X	CALIBRATED ANGLE	Angle Difference	X % Difference
-5	0.26507717	0.2619759	-5.013	0.013	1.1699502
-4	0.26532291	0.26173636	-3.889	0.111	1.35176715
-3	0.26475806	0.26051754	-2.977	0.023	1.60165967
-2	0.26554158	0.26220818	-2.125	0.125	1.25607285
-1	0.26469231	0.26163475	-0.9976	0.0024	1.15513717
0	0.2648899	0.26147008	0.1185	0.1185	1.29103287
1	0.26507358	0.26274165	0.99788	0.00212	0.87972867
2	0.26481118	0.26459853	1.908	0.092	0.08030137
3	0.26439052	0.26437015	3.039	0.039	0.00770505
4	0.26518215	0.27131254	3.981	0.019	2.31176687
5	0.26515759	0.27126343	5.206	0.206	2.30272106
6	0.26544316	0.27555841	5.9705	0.0295	3.81070088
-5	0.30008337	0.29543526	-4.997	0.003	1.54894039
-4	0.3007079	0.29766971	-4.053	0.053	1.01034686
-3	0.3004684	0.29625409	-2.846	0.154	1.40258162
-2	0.30061477	0.296241	-1.9896	0.0104	1.45494093
-1	0.30023613	0.29543177	-1.004	0.004	1.60019508
0	0.30053062	0.29964959	-0.091	0.091	0.29315864
1	0.30021511	0.29629037	1.001	0.001	1.30730965
2	0.30055141	0.3020306	1.921	0.079	0.49215954
3	0.29957054	0.30277494	3.09	0.09	1.06966512
4	0.30026045	0.30883693	4.23	0.23	2.85634722
5	0.2999669	0.30899709	4.889	0.111	3.0103945
6	0.29935007	0.31149122	6.2	0.2	4.05583392
-5	0.33781195	0.33103523	-5.013	0.013	2.00606283
-4	0.33783959	0.33154321	-3.888	0.112	1.86372124
-3	0.33764471	0.33385295	-2.965	0.035	1.12300352
-2	0.33746468	0.33049924	-1.944	0.056	2.06404389
-1	0.33782227	0.3361555	-1.037	0.037	0.49338794
0	0.33786784	0.33698174	-0.123	0.123	0.32965667
1	0.33787817	0.33725878	1.039	0.039	0.18331802
2	0.33840408	0.34005809	1.998	0.002	0.48876627
3	0.33861794	0.34611675	3.037	0.037	2.21453438
4	0.33779804	0.3486671	4.32	0.32	3.21762102
5	0.33786715	0.35165497	4.95	0.05	4.08084063
6	0.33737456	0.35312697	6.103	0.103	4.66911618
-5	0.36936742	0.36484632	-4.995	0.005	1.22401028
-4	0.36912224	0.36361324	-3.942	0.058	1.49245984
-3	0.3696089	0.36409248	-2.931	0.069	1.49250252
-2	0.36923632	0.36155338	-2.114	0.114	2.08076611
-1	0.37002864	0.36684095	-0.9156	0.0844	0.86147213
0	0.3700547	0.36725096	-0.0529	0.0529	0.75765544
1	0.37028942	0.36552042	1.007	0.007	1.28791266
2	0.36989523	0.36894668	1.839	0.161	0.25643067
3	0.3698796	0.37124174	2.87	0.13	0.36826666
4	0.37052177	0.37356432	3.209	0.209	0.82115315
5	0.36956438	0.3731039	5.1418	0.1418	0.95775437
6	0.37034436	0.37357425	5.808	0.192	0.87213134

## APPENDIX D. PROGRAM "NEW\_READ\_ZOCI"

```

10  * Program: NEW_READ_ZOCI
20  * Description: Reads specified data compiled from program BIR (BIR_ZOC),
30  * by Plot Read/Read
40  * modified by David Myers
50  * modified 5 May 1992
60  * modified 23 Feb 1993 by Jeff Austin for 3-point parameter output
70  * to determine dimensions, velocity and deviation angle during flight
80  * however, Program will also determine (range calculated from) data
90  * space.
100 .....
110 CLEAR SCREEN
120 ERASED IS CBI
130 *Variable definition and dimension
140 CBI Plot_Labels/ REAL (x,Xf,Ya,Yf,Dx,Dy,Title#501,Label#501,Label#
150 501
160 BIR_ZOC Disk device for BIR_ZOC, Sample rate, Sample size, Port size
170 BIR_ZOC File Name, Sample size, Sample
180 BIR_ZOC
190 *Variable initialization
200 CBI = 11.896 * Standard day atmosphere pressure
210 CBI = 49153 * Conversion from in Hg to psi
220 CBI = 1.5 * Ratio of specific heat
230 CBI = 0.0001 * Sub-Airplane flying
240 allocated=0
250 *Dimension string variable for data location
260 BIR_Data_disc#123
270 BIR_Data_disc#23
280
290 .....
300 *HOT KEY ROUTINES AND INITIAL SCREEN DISPLAY
310 .....
320
330 ON KEY 1 LABEL "ZOC" INPUT * GOTO Input
340 ON KEY 3 LABEL "PRINT" DATA * GOTO Print
350 ON KEY 4 LABEL "PL" PLOT * GOTO Pl
360 ON KEY 6 LABEL " " * GOTO Hold
370 ON KEY 7 LABEL " " * GOTO Hold
380 ON KEY 8 LABEL "EXIT" FROM * GOTO Hold
390
400 .....
410 *INITIAL SCREEN DISPLAY
420 .....
430
440
450 *
460 CLEAR SCREEN
470 PRINT
480 PRINT "READ ZOC DATA AND DISPLAY AS SHOWN"
490 PRINT
500 PRINT "Input ZOC information and read data" F1
510 PRINT "Print data to CBI or PRINTER" F2
520 PRINT "Plat Pl data/Print losses" F3
530 PRINT "Print out ZOC and Deviation angle"
540 PRINT "as Vertical Distance Traveled over Range Reads"
550 PRINT "Determines fully mixed out loss coefficient."
560 PRINT
570 PRINT "Exit Program" F4
580 PRINT
590
600 Hold:
610 GOTO Hold

```

Figure D1. Program "NEW\_READ\_ZOCI"

**Figure D1.** (cont) Program "NEW\_READ\_ZOC1"

```

2170 PRINT "*****"
2240 OPEN J:
2600 *
2610 PRINT
2620 *
2630 PRINT "PLOT1 (Part 1)"
2640 PRINT "PLOT1 = 1, 2, 3, 4, 5, 6, 7, 8, 9, 10, 11, 12, 13, 14, 15, 16, 17, 18, 19, 20, 21, 22, 23, 24, 25, 26, 27, 28, 29, 30, 31, 32, 33, 34, 35, 36, 37, 38, 39, 40, 41, 42, 43, 44, 45, 46, 47, 48, 49, 50, 51, 52, 53, 54, 55, 56, 57, 58, 59, 60, 61, 62, 63, 64, 65, 66, 67, 68, 69, 70, 71, 72, 73, 74, 75, 76, 77, 78, 79, 80, 81, 82, 83, 84, 85, 86, 87, 88, 89, 90, 91, 92, 93, 94, 95, 96, 97, 98, 99, 100"
2650 FOR I=1 TO 32
2670 PRINT USING Format$(I), PLOT1, I, Scan Number
2680 *
2690 PRINT "*****"
2700 *
2710 PRINT "*****"
2720 *
2730 PRINT "*****"
2740 *
2750 *
2760 *
2770 *
2780 *
2790 *
2800 *
2810 *
2820 *
2830 *
2840 *
2850 *
2860 *
2870 *
2880 *
2890 *
2900 *
2910 *
2920 *
2930 *
2940 *
2950 *
2960 *
2970 *
2980 *
2990 *
3000 *
3010 *
3020 *
3030 *
3040 *
3050 *
3060 *
3070 *
3080 *
3090 *
3100 *
3110 *
3120 *
3130 *
3140 *
3150 *
3160 *
3170 *
3180 *
3190 *
3200 *
3210 *
3220 *
3230 *
3240 *
3250 *
3260 *
3270 *
3280 *
3290 *
3300 *
3310 *
3320 *
3330 *
3340 *
3350 *
3360 *
3370 *
3380 *
3390 *
3400 *
3410 *
3420 *
3430 *
3440 *
3450 *
3460 *
3470 *
3480 *
3490 *
3500 *
3510 *
3520 *
3530 *
3540 *
3550 *
3560 *
3570 *
3580 *
3590 *
3600 *
3610 *
3620 *
3630 *
3640 *
3650 *
3660 *
3670 *
3680 *
3690 *
3700 *
3710 *
3720 *
3730 *
3740 *
3750 *
3760 *
3770 *
3780 *
3790 *
3800 *
3810 *
3820 *
3830 *
3840 *
3850 *
3860 *
3870 *
3880 *
3890 *
3900 *
3910 *
3920 *
3930 *
3940 *
3950 *
3960 *
3970 *
3980 *
3990 *
4000 *
4010 *
4020 *
4030 *
4040 *
4050 *
4060 *
4070 *
4080 *
4090 *
4100 *
4110 *
4120 *
4130 *
4140 *
4150 *
4160 *
4170 *
4180 *
4190 *
4200 *
4210 *
4220 *
4230 *
4240 *
4250 *
4260 *
4270 *
4280 *
4290 *
4300 *
4310 *
4320 *
4330 *
4340 *
4350 *
4360 *
4370 *
4380 *
4390 *
4400 *
4410 *
4420 *
4430 *
4440 *
4450 *
4460 *
4470 *
4480 *
4490 *
4500 *
4510 *
4520 *
4530 *
4540 *
4550 *
4560 *
4570 *
4580 *
4590 *
4600 *
4610 *
4620 *
4630 *
4640 *
4650 *
4660 *
4670 *
4680 *
4690 *
4700 *
4710 *
4720 *
4730 *
4740 *
4750 *
4760 *
4770 *
4780 *
4790 *
4800 *
4810 *
4820 *
4830 *
4840 *
4850 *
4860 *
4870 *
4880 *
4890 *
4900 *
4910 *
4920 *
4930 *
4940 *
4950 *
4960 *
4970 *
4980 *
4990 *
5000 *
5010 *
5020 *
5030 *
5040 *
5050 *
5060 *
5070 *
5080 *
5090 *
5100 *
5110 *
5120 *
5130 *
5140 *
5150 *
5160 *
5170 *
5180 *
5190 *
5200 *
5210 *
5220 *
5230 *
5240 *
5250 *
5260 *
5270 *
5280 *
5290 *
5300 *
5310 *
5320 *
5330 *
5340 *
5350 *
5360 *
5370 *
5380 *
5390 *
5400 *
5410 *
5420 *
5430 *
5440 *
5450 *
5460 *
5470 *
5480 *
5490 *
5500 *
5510 *
5520 *
5530 *
5540 *
5550 *
5560 *
5570 *
5580 *
5590 *
5600 *
5610 *
5620 *
5630 *
5640 *
5650 *
5660 *
5670 *
5680 *
5690 *
5700 *
5710 *
5720 *
5730 *
5740 *
5750 *
5760 *
5770 *
5780 *
5790 *
5800 *
5810 *
5820 *
5830 *
5840 *
5850 *
5860 *
5870 *
5880 *
5890 *
5900 *
5910 *
5920 *
5930 *
5940 *
5950 *
5960 *
5970 *
5980 *
5990 *
6000 *
6010 *
6020 *
6030 *
6040 *
6050 *
6060 *
6070 *
6080 *
6090 *
6100 *
6110 *
6120 *
6130 *
6140 *
6150 *
6160 *
6170 *
6180 *
6190 *
6200 *
6210 *
6220 *
6230 *
6240 *
6250 *
6260 *
6270 *
6280 *
6290 *
6300 *
6310 *
6320 *
6330 *
6340 *
6350 *
6360 *
6370 *
6380 *
6390 *
6400 *
6410 *
6420 *
6430 *
6440 *
6450 *
6460 *
6470 *
6480 *
6490 *
6500 *
6510 *
6520 *
6530 *
6540 *
6550 *
6560 *
6570 *
6580 *
6590 *
6600 *
6610 *
6620 *
6630 *
6640 *
6650 *
6660 *
6670 *
6680 *
6690 *
6700 *
6710 *
6720 *
6730 *
6740 *
6750 *
6760 *
6770 *
6780 *
6790 *
6800 *
6810 *
6820 *
6830 *
6840 *
6850 *
6860 *
6870 *
6880 *
6890 *
6900 *
6910 *
6920 *
6930 *
6940 *
6950 *
6960 *
6970 *
6980 *
6990 *
7000 *
7010 *
7020 *
7030 *
7040 *
7050 *
7060 *
7070 *
7080 *
7090 *
7100 *
7110 *
7120 *
7130 *
7140 *
7150 *
7160 *
7170 *
7180 *
7190 *
7200 *
7210 *
7220 *
7230 *
7240 *
7250 *
7260 *
7270 *
7280 *
7290 *
7300 *
7310 *
7320 *
7330 *
7340 *
7350 *
7360 *
7370 *
7380 *
7390 *
7400 *
7410 *
7420 *
7430 *
7440 *
7450 *
7460 *
7470 *
7480 *
7490 *
7500 *
7510 *
7520 *
7530 *
7540 *
7550 *
7560 *
7570 *
7580 *
7590 *
7600 *
7610 *
7620 *
7630 *
7640 *
7650 *
7660 *
7670 *
7680 *
7690 *
7700 *
7710 *
7720 *
7730 *
7740 *
7750 *
7760 *
7770 *
7780 *
7790 *
7800 *
7810 *
7820 *
7830 *
7840 *
7850 *
7860 *
7870 *
7880 *
7890 *
7900 *
7910 *
7920 *
7930 *
7940 *
7950 *
7960 *
7970 *
7980 *
7990 *
8000 *
8010 *
8020 *
8030 *
8040 *
8050 *
8060 *
8070 *
8080 *
8090 *
8100 *
8110 *
8120 *
8130 *
8140 *
8150 *
8160 *
8170 *
8180 *
8190 *
8200 *
8210 *
8220 *
8230 *
8240 *
8250 *
8260 *
8270 *
8280 *
8290 *
8300 *
8310 *
8320 *
8330 *
8340 *
8350 *
8360 *
8370 *
8380 *
8390 *
8400 *
8410 *
8420 *
8430 *
8440 *
8450 *
8460 *
8470 *
8480 *
8490 *
8500 *
8510 *
8520 *
8530 *
8540 *
8550 *
8560 *
8570 *
8580 *
8590 *
8600 *
8610 *
8620 *
8630 *
8640 *
8650 *
8660 *
8670 *
```

**Figure D1.** (cont) Program "NEW READ ZOC1"

```

610 ***** DAT INFORMATION *****
620 *****
630 *****
640 Input: 1
650 1
660 IF Allocated=0 THEN GO500 Deallocate
670 1
680 *****
690 *****
700 *****
710 *****
720 *****
730 *****
740 *****
750 *****
760 *****
770 *****
780 *****
790 *****
800 *****
810 *****
820 *****
830 *****
840 *****
850 *****
860 *****
870 *****
880 *****
890 *****
900 *****
910 *****
920 *****
930 *****
940 *****
950 *****
960 *****
970 *****
980 *****
990 *****
1000 *****
1010 *****
1020 *****
1030 *****
1040 *****
1050 *****
1060 *****
1070 *****
1080 *****
1090 *****
1100 *****
1110 *****
1120 *****
1130 *****
1140 *****
1150 *****
1160 *****
1170 *****
1180 *****
1190 *****
1200 *****
1210 *****
1220 *****
1230 *****
1240 *****
1250 *****

```

**Figure D1.** (cont) Program "NEW\_READ\_ZOC1"

[illegible]

**Figure D1.** (cont) Program "NEW\_READ\_ZOC1"

[illegible]

**Figure D1.** (cont) Program "NEW\_READ\_ZOC1"

```

5615 IF X_val(1) < X_val(500) THEN X_val(1)=X_val(500)
5616 X_upper=X_val(6)
5617 X_lower=X_val(3)
5618 Phi_upper=Phi_4(1)
5619 Phi_lower=Phi_5(1)
5620 END IF
5621 IF X_val(1) < X_val(400) THEN X_val(1)=X_val(400)
5622 X_upper=X_val(5)
5623 X_lower=X_val(4)
5624 Phi_upper=Phi_5(1)
5625 Phi_lower=Phi_4(1)
5626 END IF
5627 IF X_val(1) < X_val(500) THEN X_val(1)=X_val(500)
5628 X_upper=X_val(6)
5629 X_lower=X_val(3)
5630 Phi_upper=Phi_5(1)
5631 Phi_lower=Phi_4(1)
5632 END IF
5633 IF X_val(1) < X_val(7) AND X_val(1) < X_val(8) THEN
5634 X_upper=X_val(8)
5635 X_lower=X_val(7)
5636 Phi_upper=Phi_7(1)
5637 Phi_lower=Phi_7(1)
5638 END IF
5639
5640 ! Lagrange interpolation to find the deviation angle
5641 Yank_val()
5642 Yank=0
5643 X_interp(1)=X_lower
5644 X_interp(2)=X_upper
5645 F_interp(1)=Phi_lower
5646 F_interp(2)=Phi_upper
5647 FOR I=1 TO N_pts
5648 J=I
5649 FOR K=1 TO N_pts
5650 IF J=K THEN
5651 GOTO 5654
5652 END IF
5653 Z=2*(X_val(X_interp(I))/Y_val(X_interp(I)) - X_val(X_interp(J))/Y_val(X_interp(J)))
5654 Yank=Yank+Z*(F_interp(I) - F_interp(J))
5655 NEXT J
5656 NEXT I
5657 Phi_dev(J)=R_0*Yank
5658 NEXT I
5659
5660 !.....
5661 ! Phi loss coefficient calculation in this position
5662 !.....
5663 ! Phi loss calculated above.
5664 FOR I=1 TO Scan_num
5665 Plot_P_val(I),Y(I),Pen(I)
5666 NEXT I
5667 PAUSE
5668 CLEAR SCREEN
5669 Print results to Thin-2a
5670 PRINTED IS OK
5671 INPUT "Deviation angle and X_val data to CRT or Printer (0-CRT 1-Printer) :>
5672 IF Dev=1 THEN PRINTER IS OK
5673 CLEAR SCREEN
5674

```

**Figure D1 (cont) Program "NEW\_READ\_ZOC1"**

[illegible]

**Figure D1.** (cont) Program "NEW READ ZOC1"

```

772 I1 = X_val(1) + 2*(1/Gamma+1)*H1+X_val(1)*2*(1/Gamma+Gamma-1)*H1
5748 I3_dend(I)=X1_ref(1)*2*(1-X1_ref(1))^2*(1/(Gamma-1))
5750 I3_array(I)=I3_num(1)/I3_dend(I)
5751 I
5752 NEXT I
5753 ! Begin calling subprograms to determine upper interval of integration
5754 Lcpoint1=1
5755 Hcpoint1=33
5756 CALL checkflus(Lcpoint1,Hcpoint1,I3_array(*),Y(*),I1,Int_Posit1,Int_Pos2,
& Value2,High_1,Low_1)
5757 PRINT "VALUE1="&Value1
5758 PRINT "VALUE2="&Value2
5759 PRINT "I1="&High_1
5760 PRINT "I1="&Low_1
5761 !Returns the index values to interpolate between when calculating I1,I2,I3
5762 !Interpolate to find proper traverse position for one blade space.
5763 Xa,I=1:8
5764 PAUSE
5765 CALL Interpolate(Value1,Value2,Posit1,Posit2,Probe_posit,Xa,I)
5766 PRINT "Probe position for one blade space ="&(Probe_posit)
5767 PAUSE
5768 ! BEGIN VALUES TO CHECK SUBPROGRAMS
5769 I1=1.6345
5770 ! =====
5771 ! Begin calculations of I1,I2,I3 by calling Dat_int subprogram
5772 ! Define the upper and lower points of the integrals
5773 Lcpoint1=1
5774 CALL Dat_int(Lcpoint1,High_1,I1_array(*),Y(*),I1_int_lo,I1_int_hi)
5775 CALL Dat_int(Lcpoint1,Low_1,I1_array(*),Y(*),I1_int_lo)
5776 CALL Interpolate(Value1,Value2,I1_int_lo,I1_int_hi,I3_int,Xa,I)
5777 PRINT "I1_INT="&I1_int
5778 PAUSE
5779 I
5780 CALL Dat_int(Lcpoint1,High_1,I2_array(*),Y(*),I2_int_hi)
5781 CALL Dat_int(Lcpoint1,Low_1,I2_array(*),Y(*),I2_int_lo)
5782 CALL Interpolate(Value1,Value2,I2_int_lo,I2_int_hi,I3_int,Xa,I)
5783 PRINT "I2_INT="&I2_int
5784 PAUSE
5785 I
5786 CALL Dat_int(Lcpoint1,High_1,I3_array(*),Y(*),I3_int_hi)
5787 CALL Dat_int(Lcpoint1,Low_1,I3_array(*),Y(*),I3_int_lo)
5788 CALL Interpolate(Value1,Value2,I3_int_lo,I3_int_hi,I3_int,Xa,I)
5789 PRINT "I3_INT="&I3_int
5790 PAUSE
5791 REAL P1_ref_avg
5792 REAL X_ref_avg
5793 REAL Q_ref_avg
5794 REAL P_ref_avg
5795 X_ref_avg=0
5796 P1_ref_avg=0
5797 Q_ref_avg=0
5798 P_ref_avg=0
5799 FOR J=1 TO High_1
5800 X_ref_avg=X1_ref(I)+X_ref_avg
5801 P1_ref_avg=P1(I)+P1_ref_avg
5802 Q_ref_avg=Q_ref(I)+Q_ref_avg
5803 P_ref_avg=P_ref(I)+P_ref_avg
5804 NEXT J
5805 X_ref_avg=X_ref_avg/High_1
5806 P1_ref_avg=P1_ref_avg/High_1
5807 Q_ref_avg=Q_ref_avg/High_1
5808 P_ref_avg=P_ref_avg/High_1
5809 I
5810 !====using I1,I2,I3 calculate A,B,C,D,E
5811 A=(I2_int/I1_int)*X_ref_avg
5812 B=(I3_int/I1_int)*X_ref_avg
5813 C=(Gamma+1)/(Gamma-1)*B

```

Figure D1. (cont) Program "NEW\_READ\_ZOCI"

```

6216 B1=2+SQRT(1+1+1-(12+Ganna)/(Ganna+13)*A1^2)/B1^2
6217 E1=0+2*A1^2+1+1-(2+Ganna)/(Ganna+13)*A1^2+2
6219 X3_super=SQRT(1-D1+SQRT(D1^2-4+C1+E1))/(2+C1)
6220 X3_sub=SQRT(1-D1+SQRT(D1^2-4+C1+E1))/(2+C1)
6221 PRINT "X3 SUB" "X3 SUB"
6222 X3_mixed=X3_sub
6223 DEG
6224 Beta3_mixed=BN(A1/X3_mixed)
6225 P13=P1_ref_avg*X_ref_avg+1-X_ref_avg^2/(1+(Ganna+13)*E1_sub+X3^2)
6226 P13_mixed=2/(1+(Ganna+13)*DOS(Beta3_mixed))
6227 P13=1+1+int(P1_ref_avg*X_ref_avg+1-X_ref_avg^2)/(1+(Ganna+13)*DOS(Beta3_mixed)+X3_mixed^2)/(1+(Ganna+13))
6228 U_mixed=P1_ref_avg/P13/(1+U_ref_avg)
6229 IFB=Device In print results (@PCRE INT INTEGER) 5m
6230 IF U=1 THEN PRINTER IS 727
6231 CLEAR SCREEN
6232 PRINT "14 UPPER = "P13_mixed
6233 PRINT "14 LOWER = "U_mixed
6234 PRINT "X3_mixed = "X3_mixed
6235 PRINT "P_ref_avg = "P1_ref_avg
6236 PRINT "P13_mixed = "P13
6237 PRINT "Beta3_mixed = "Beta3_mixed
6238 PRINT "U_mixed = "U_mixed
6239 PAUSE
6240 I
6241 Plot statistic that was calculated by Neutronian Iteration
6242 I
6243 CLEAR SCREEN
6244 PRINTER IS CRT
6245 CALL Plot
6246 FOR I=1 TO Scan_max
6247   PLOT P_exit(I),Y(I),Pen2(I)
6248 NEXT I
6249 FOR I=1 TO Scan_max
6250   PLOT P_at_p(I),Y(I),Pen2(I)
6251 NEXT I
6252 PUSE
6253 Deallocate all real variables
6254 I
6255 DEALLOCATE Pen2(*)
6256 DEALLOCATE P_inf(*)
6257 DEALLOCATE P_exit(*)
6258 DEALLOCATE P_ref(*)
6259 DEALLOCATE P_inf(*)
6260 DEALLOCATE P_exit(*)
6261 DEALLOCATE M1(*)
6262 DEALLOCATE M2(*)
6263 DEALLOCATE M3(*)
6264 DEALLOCATE M4(*)
6265 DEALLOCATE D1(*)
6266 DEALLOCATE P1(*)
6267 DEALLOCATE Y1(*)
6268 *****
6269 Deallocate added variables
6270 DEALLOCATE P2_inf(*)
6271 DEALLOCATE P_at_pi(*)
6272 DEALLOCATE P3_inf(*)
6273 DEALLOCATE Pitch1(*)
6274 DEALLOCATE Pitch_pi(*)
6275 DEALLOCATE X_vel_pi(*)
6276 DEALLOCATE X_vel(*)
6277 DEALLOCATE Beta_pi(*)
6278 DEALLOCATE Ganna_pi(*)
6279 DEALLOCATE X_interpi(*)

```

Figure D1. (cont) Program "NEW\_READ\_ZOC1"



<pre> 6770 10000 6775 10000 6800 10000 6810 LABEL Y_Label3 6820 10000 6830 10000 6840 VIEWPORT 10,90,60,10,10,90 6850 ERASE 6900 STOPX=X,Xf,Xo,Xf 6910 AX=X+range/Dx,Xf,Xo,Xo,Xf 6920 AX=X+range/Dx,Xf,Xo,Xo,Xf 6930 STOPX=X,Xf,Xo,Xf 6940 10000 6950 10000 6960 10000 6970 10000 6980 10000 6990 10000 7000 10000 7010 10000 7020 10000 7030 10000 7040 10000 7050 10000 7060 10000 7070 10000 7080 10000 7090 10000 7100 10000 7110 10000 7120 10000 7130 10000 7140 10000 7150 10000 7160 10000 7170 10000 </pre>	<pre> 7180 10000 7190 10000 7200 10000 7210 10000 7220 10000 7230 10000 7240 10000 7250 10000 7260 10000 7270 10000 7280 10000 7290 10000 7300 10000 7310 10000 7320 10000 7330 10000 7340 10000 7350 10000 7360 10000 7370 10000 7380 10000 7390 10000 7400 10000 7410 10000 7420 10000 7430 10000 7440 10000 7450 10000 7460 10000 7470 10000 7480 10000 7490 10000 7500 10000 7510 10000 7520 10000 7530 10000 7540 10000 7550 10000 7560 10000 7570 10000 7580 10000 7590 10000 7600 10000 7610 10000 7620 10000 7630 10000 7640 10000 7650 10000 7660 10000 7670 10000 7680 10000 7690 10000 7700 10000 7710 10000 7720 10000 7730 10000 7740 10000 7750 10000 7760 10000 7770 10000 7780 10000 7790 10000 7800 10000 7810 10000 7820 10000 7830 10000 7840 10000 7850 10000 7860 10000 7870 10000 7880 10000 7890 10000 7900 10000 7910 10000 7920 10000 7930 10000 7940 10000 7950 10000 7960 10000 7970 10000 7980 10000 7990 10000 8000 10000 8010 10000 8020 10000 8030 10000 8040 10000 8050 10000 8060 10000 8070 10000 8080 10000 8090 10000 8100 10000 8110 10000 8120 10000 8130 10000 8140 10000 8150 10000 8160 10000 8170 10000 8180 10000 8190 10000 8200 10000 8210 10000 8220 10000 8230 10000 8240 10000 8250 10000 8260 10000 8270 10000 8280 10000 8290 10000 8300 10000 8310 10000 8320 10000 8330 10000 8340 10000 8350 10000 8360 10000 8370 10000 8380 10000 8390 10000 8400 10000 8410 10000 8420 10000 8430 10000 8440 10000 8450 10000 8460 10000 8470 10000 8480 10000 8490 10000 8500 10000 8510 10000 8520 10000 8530 10000 8540 10000 8550 10000 8560 10000 8570 10000 8580 10000 8590 10000 8600 10000 8610 10000 8620 10000 8630 10000 8640 10000 8650 10000 8660 10000 8670 10000 8680 10000 8690 10000 8700 10000 8710 10000 8720 10000 8730 10000 8740 10000 8750 10000 8760 10000 8770 10000 8780 10000 8790 10000 8800 10000 8810 10000 8820 10000 8830 10000 8840 10000 8850 10000 8860 10000 8870 10000 8880 10000 8890 10000 8900 10000 8910 10000 8920 10000 8930 10000 8940 10000 8950 10000 8960 10000 8970 10000 8980 10000 8990 10000 9000 10000 9010 10000 9020 10000 9030 10000 9040 10000 9050 10000 9060 10000 9070 10000 9080 10000 9090 10000 9100 10000 9110 10000 9120 10000 9130 10000 9140 10000 9150 10000 9160 10000 9170 10000 9180 10000 9190 10000 9200 10000 9210 10000 9220 10000 9230 10000 9240 10000 9250 10000 9260 10000 9270 10000 9280 10000 9290 10000 9300 10000 9310 10000 9320 10000 9330 10000 9340 10000 9350 10000 9360 10000 9370 10000 9380 10000 9390 10000 9400 10000 9410 10000 9420 10000 9430 10000 9440 10000 9450 10000 9460 10000 9470 10000 9480 10000 9490 10000 9500 10000 9510 10000 9520 10000 9530 10000 9540 10000 9550 10000 9560 10000 9570 10000 9580 10000 9590 10000 9600 10000 9610 10000 9620 10000 9630 10000 9640 10000 9650 10000 9660 10000 9670 10000 9680 10000 9690 10000 9700 10000 9710 10000 9720 10000 9730 10000 9740 10000 9750 10000 9760 10000 9770 10000 9780 10000 9790 10000 9800 10000 9810 10000 9820 10000 9830 10000 9840 10000 9850 10000 9860 10000 9870 10000 9880 10000 9890 10000 9900 10000 9910 10000 9920 10000 9930 10000 9940 10000 9950 10000 9960 10000 9970 10000 9980 10000 9990 10000 10000 10000 </pre>
--	--

Figure D1. (cont) - Program "NEW\_READ\_ZOC1"

```

7700 SUB ROUTINE4 (INTEGER Equipoint, High1, High2, Value1, Value2, INTEGER High3, Low1)
7710 GOTO 8050
7720 DIM A(100)
7730 DIM B(100)
7740 DIM C(100)
7750 DIM Dint(100)
7760 DIM Distint(100)
7770 HLT A=0
7780 HLT B=0
7790 HLT C=0
7800 HLT Dist=0
7810 HLT Distint=0
7811 L3=0
7820 H=Equipoint+1
7821 Dist=1
7830 FOR I=Equipoint+1 TO H
7840 C(I)=1/(Pos(I+1)-Pos(I-1))*(C(I+1)-C(I-1))/Pos(I+1)-Pos(I-1)
7850 B(I)=C(I+1)-C(I-1)/Pos(I)-Pos(I-1)/(Pos(I)-Pos(I-1)+1)
7860 C(I)=B(I)+B(I)*Pos(I)*Pos(I-1)/B(I)+Pos(I)
7870 HLT
7880 Dist(I)=A(I)*Pos(2)+3-Pos(1)+3/3.0+B(I)*Pos(2)+3-Pos(1)+3/3.0+C(I)*Pos(2)+3-Pos(1)+3/3.0+Dint(I)+3-Pos(1)+3/3.0
7890 Distint(I)=N*(Pos(N)+3-Pos(N)+3/3.0+B(I)+Pos(N)+3-Pos(N)+3/3.0+C(I)+3-Pos(N)+3/3.0+Dint(I))
7900 FOR I=Equipoint+1 TO H
7910 Dist(I)=A(I)+B(I)+C(I)+Dint(I)+3-Pos(I)+3/3.0+B(I)+Pos(I)+3-Pos(I)+3/3.0+C(I)+Pos(I)+3-Pos(I)+3/3.0+Dint(I)+3-Pos(I)+3/3.0
7920 NEXT I
7930 FOR I=1 TO N
7940 I1=Int=14-Int+Dint(I)
7950 IF I1=0 THEN
7960 Pos(1)=Pos(I)
7970 Pos(1)=Pos(I-1)
7980 Value2=14-Int
7990 Value1=14-Int-Dint(I)
8000 High1=I1
8010 Low1=I1-1
8020 GOTO 8040
8030 END IF
8040 NEXT I
8050 Pos(1)=Pos(I)
8060 Pos(1)=Pos(I-1)
8070 Value2=14-Int
8080 Value1=14-Int-Dint(I)
8090 High1=I1
8100 Low1=I1-1
8110 RETURN

```

Figure D1. (cont) Program "NEW\_READ\_ZOC1"

```

0000 0000 Integrate(Erfi(x)*log(1+x),x,0,1)
0001 0001 DO SE 1
0002 0002 Goto 100
0003 0003 Integrate E
0004 0004 Integrate E
0005 0005 DIF 1
0006 0006 DIF 1
0007 0007 DIF 1
0008 0008 DIF 1
0009 0009 DIF 1
0010 0010 DIF 1
0011 0011 DIF 1
0012 0012 DIF 1
0013 0013 DIF 1
0014 0014 DIF 1
0015 0015 DIF 1
0016 0016 DIF 1
0017 0017 DIF 1
0018 0018 DIF 1
0019 0019 DIF 1
0020 0020 DIF 1
0021 0021 DIF 1
0022 0022 DIF 1
0023 0023 DIF 1
0024 0024 DIF 1
0025 0025 DIF 1
0026 0026 DIF 1
0027 0027 DIF 1
0028 0028 DIF 1
0029 0029 DIF 1
0030 0030 DIF 1
0031 0031 DIF 1
0032 0032 DIF 1
0033 0033 DIF 1
0034 0034 DIF 1
0035 0035 DIF 1
0036 0036 DIF 1
0037 0037 DIF 1
0038 0038 DIF 1
0039 0039 DIF 1
0040 0040 DIF 1
0041 0041 DIF 1
0042 0042 DIF 1
0043 0043 DIF 1
0044 0044 DIF 1
0045 0045 DIF 1
0046 0046 DIF 1
0047 0047 DIF 1
0048 0048 DIF 1
0049 0049 DIF 1
0050 0050 DIF 1
0051 0051 DIF 1
0052 0052 DIF 1
0053 0053 DIF 1
0054 0054 DIF 1
0055 0055 DIF 1
0056 0056 DIF 1
0057 0057 DIF 1
0058 0058 DIF 1
0059 0059 DIF 1
0060 0060 DIF 1
0061 0061 DIF 1
0062 0062 DIF 1
0063 0063 DIF 1
0064 0064 DIF 1
0065 0065 DIF 1
0066 0066 DIF 1
0067 0067 DIF 1
0068 0068 DIF 1
0069 0069 DIF 1
0070 0070 DIF 1
0071 0071 DIF 1
0072 0072 DIF 1
0073 0073 DIF 1
0074 0074 DIF 1
0075 0075 DIF 1
0076 0076 DIF 1
0077 0077 DIF 1
0078 0078 DIF 1
0079 0079 DIF 1
0080 0080 DIF 1
0081 0081 DIF 1
0082 0082 DIF 1
0083 0083 DIF 1
0084 0084 DIF 1
0085 0085 DIF 1
0086 0086 DIF 1
0087 0087 DIF 1
0088 0088 DIF 1
0089 0089 DIF 1
0090 0090 DIF 1
0091 0091 DIF 1
0092 0092 DIF 1
0093 0093 DIF 1
0094 0094 DIF 1
0095 0095 DIF 1
0096 0096 DIF 1
0097 0097 DIF 1
0098 0098 DIF 1
0099 0099 DIF 1
0100 0100 DIF 1

```

**Figure D1.** (cont) Program "NEW\_READ\_ZOC1"

## APPENDIX E. MIXED-OUT LOSS CALCULATION

The calculation of the total pressure loss coefficient in the fan-blade cascade model required the calculation of fully-mixed-out-flow conditions. This requirement was difficult due to the probe not traversing parallel to the trailing edge of the blades, and the use of uneven spacings. Figure E1 shows the fully-mixed-out control volume for the analysis, and the location of the traverse in the fan blade cascade model.

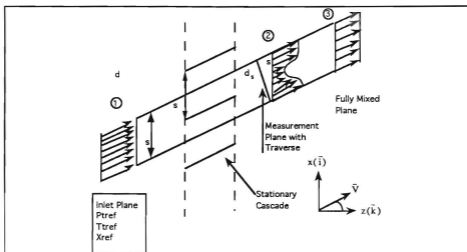


Figure E1. Fully-Mixed-Out Control Volume

The equations for the analysis, reported by Armstrong [Ref. 12], were programmed in HP Basic and are part of the data reduction program "NEW\_READ\_ZOC1" listed in Appendix D. The analysis required that the probe data be taken over a single blade space. Due to the probe traverse not traversing parallel to the trailing edge, it was required that the program calculate when the

probe had measured the same integrated mass flux at position 2 as had entered at position 1( where nozzle free-stream conditions were known). The integral in equation 1 was programmed as a subprogram labeled "Mass\_flux".

$$1 = \int_0^{\frac{d_s}{d_1}} \frac{X_2(1-X_2)^{\frac{1}{\gamma-1}}}{X_{ref}(1-X_{ref})^{\frac{1}{\gamma-1}}} \cdot \frac{P_{T2}}{P_{T1}} \cdot \cos \beta_2 d\left(\frac{x}{d_1}\right) \quad (1)$$

where  $d_1$  is the staggered passage width of 1.656 inches and  $d_s$  is the blade traverse distance required for the analysis. By computing the integral at every point in the traverse, the distance  $d_s$  was determined where the integral became unity. Once the proper blade space distance was known the following equations could be calculated using the subprogram "Dat\_int" which was an integration scheme designed to integrate a function over non-equispaced points.

$$\hat{I}_1 = \int_0^1 \frac{X_2(1-X_2)^{\frac{1}{\gamma-1}}}{X_{ref}(1-X_{ref})^{\frac{1}{\gamma-1}}} \cdot \frac{P_{T2}}{P_{Tref}} \cdot \cos \beta_2 d\left(\frac{x}{s}\right) \quad (2)$$

$$\hat{I}_2 = \int_0^1 \frac{X_2^2(1-X_2^2)^{\frac{1}{\gamma-1}}}{X_{ref}^2(1-X_{ref}^2)^{\frac{1}{\gamma-1}}} \cdot \frac{P_{T2}}{P_{Tref}} \cdot \cos \beta_2 \sin \beta_2 d\left(\frac{x}{s}\right) \quad (3)$$

$$\hat{I}_3 = \int_0^1 \frac{\left[ (1-X_2^2)^{\frac{\gamma}{\gamma-1}} + \left( \frac{2\gamma}{\gamma-1} \right) \cdot X_2^2 (1-X_2^2)^{\frac{1}{\gamma-1}} \cdot \cos^2 \beta_2 \right]}{X_{ref}^2 (1-X_{ref}^2)^{\frac{1}{\gamma-1}}} \cdot \frac{P_{T2}}{P_{Tref}} \cdot d\left(\frac{x}{s}\right) \quad (4)$$

$$\hat{A} = X_{ref} \cdot \frac{\hat{I}_2}{\hat{A}} = X_3 \sin \beta_3 \quad (5)$$

$$\hat{B} = X_{ref} \cdot \frac{\hat{I}_3}{\hat{A}} = \frac{\left[ (1-X_3^2) + \left( \frac{2\gamma}{\gamma-1} \right) X_3^2 \cos^2 \beta_3 \right]}{X_3 \cos \beta_3} \quad (6)$$

$$C = \left( \frac{\gamma+1}{\gamma-1} \right)^2 \quad (7)$$

$$D = 2 \left( \frac{\gamma+1}{\gamma-1} \right) \left[ 1 - \left( \frac{2\gamma}{\gamma-1} \right) \hat{A}^2 \right] - \hat{B}^2 \quad (8)$$

$$E = \left[ 1 - \left( \frac{2\gamma}{\gamma-1} \right) \hat{A}^2 \right]^2 + \hat{A}^2 \hat{B}^2 \quad (9)$$

$$X_3^2 = \frac{-D \pm \sqrt{D^2 - 4CE}}{2C} \quad (10)$$

where the subsonic root of  $X_3$  is chosen

$$\beta_3 = \sin^{-1} \left( \frac{\hat{A}}{X_3} \right) \quad (11)$$

$$P_{T3} = \frac{X_{ref} \left( 1 - X_{ref}^2 \right)^{\frac{1}{\gamma-1}} P_{Tref} \hat{I}_1}{X_3 \left( 1 - X_3 \right)^{\frac{1}{\gamma-1}} \cos \beta_3} \quad (12)$$

The fully-mixed-out loss coefficient could be then be calculated using the inlet total pressure, the fully-mixed-out total pressure, and inlet static pressure in Equation 13.

$$\varpi = \frac{P_{tref} - P_{t3}}{P_{tref} - P_{staticref}} \quad (13)$$

When the above procedure was followed using the baseline test data, the values obtained for  $d_s$  were significantly greater than 1.656 inches. In reducing the baseline data, the fully-mixed-out condition was calculated using Eq. (2) - Eq.(12), with the full survey distance (s), which was 1.656 inches.

## APPENDIX F. SELECTED RAW DATA

Data Print Out for Log # 1, Run # 2, F1167P141424							
Period between samples (sec): .0030303030303							
Sample collection rate (Hz): 330							
Number of samples per port: 10							
Length of data run (sec): 31							
The scan type is: 3							
Number of scans/traverses: 31							
Increment of traverse: .0625 inches							
Atmospheric pressure is: 14.72 psia							
Tunnel Pressure Ratio is: 2.11030215726							
Scan	1	24	25	29	30	31	32
1	15.410	47.191	45.052	15.463	32.632	53.780	51.635
2	15.410	47.276	45.023	15.483	32.642	53.714	51.607
3	15.390	47.257	44.976	15.473	32.662	53.790	51.550
4	15.443	46.982	44.769	15.403	32.622	53.741	51.704
5	15.399	46.982	44.712	15.533	32.582	53.650	51.170
6	15.399	46.906	44.562	15.543	32.562	53.649	51.112
7	15.377	47.001	44.619	15.483	32.562	53.700	51.190
8	15.356	47.087	44.741	15.503	32.602	53.604	51.200
9	15.421	47.096	44.684	15.513	32.547	53.600	51.312
10	15.291	46.782	44.429	15.513	32.462	53.600	50.921
11	15.356	46.915	44.543	15.513	32.562	53.700	51.056
12	15.388	47.343	44.901	15.473	32.493	53.714	51.493
13	15.387	47.428	44.910	15.463	32.582	53.677	51.607
14	15.453	46.372	43.644	15.533	32.527	53.650	50.433
15	15.399	42.269	40.175	15.503	32.952	53.641	45.396
16	15.410	41.344	39.451	15.493	32.542	53.632	43.554
17	15.432	38.783	38.000	15.463	32.582	53.741	40.095
18	15.345	41.919	41.625	15.483	32.532	53.569	44.488
19	15.399	46.239	45.230	15.523	32.582	53.732	50.625
20	15.421	46.801	45.969	15.523	32.682	53.723	51.303
21	15.367	46.744	45.522	15.523	32.532	53.623	51.246
22	15.432	46.649	45.456*	15.453	32.502	53.641	51.265
23	15.464	46.582	45.612	15.533	32.472	53.723	51.227
24	15.356	46.497	45.597	15.543	32.512	53.706	51.189
25	15.410	46.439	45.456	15.563	32.482	53.632	50.980
26	15.464	46.420	45.569	15.513	32.522	53.700	51.084
27	15.377	46.296	45.550	15.543	32.552	53.695	51.007
28	15.443	46.382	45.662	15.533	32.482	53.632	51.036
29	15.399	46.229	45.650	15.483	32.502	53.632	51.046
30	15.399	46.373	45.901	15.593	32.512	53.669	51.151
31	15.432	46.277	46.083	15.543	32.462	53.705	51.170
32	15.443	46.105	46.206	15.543	32.622	53.695	51.131
33	15.421	46.210	46.196	15.513	32.442	53.650	51.360

Figure F1. Run 2 2/24/94 Raw Data

Portion	Boin	Sagwa	X_val	Pst	$\theta$
+0.00000	+1.105000	+1.307342	+1.335411	+34.004505	+1.720
+0.05750	+1.105751	+1.4119836	+1.337412	+34.046277	+1.800
+0.12500	+1.105312	+1.421953	+1.3371000	+34.100000	+1.750
+0.18750	+1.105462	+1.409157	+1.337118	+34.060000	+1.750
+0.25000	+1.104812	+1.405407	+1.337006	+34.000000	+1.700
+0.31250	+1.105042	+1.426961	+1.337102	+34.000000	+1.700
+0.37500	+1.105249	+1.442105	+1.337100	+34.000000	+1.700
+0.43750	+1.103393	+1.443094	+1.337000	+34.000000	+1.700
+0.50000	+1.105574	+1.444209	+1.337000	+34.000000	+1.700
+0.56250	+1.104399	+1.427623	+1.337000	+34.000000	+1.700
+0.62500	+1.104318	+1.445500	+1.338561	+34.000000	+1.700
+0.68750	+1.104315	+1.454601	+1.338561	+34.000000	+1.700
+0.75000	+1.105376	+1.463002	+1.337474	+34.000000	+1.700
+0.81250	+1.107555	+1.502941	+1.337000	+34.000000	+1.700
+0.87500	+0.991957	+1.501652	+1.297027	+34.000000	+1.700
+0.93750	+0.972361	+1.507344	+1.266494	+34.000000	+1.700
+1.00000	+0.942376	+1.456134	+1.191400	+34.000000	+1.700
+1.06250	+0.961044	+1.108796	+1.213559	+34.000000	+1.700
+1.12500	+0.996589	+1.206269	+1.300205	+34.000000	+1.700
+1.18750	+0.989762	+1.240054	+1.316300	+34.000000	+1.700
+1.25000	+0.999773	+1.239109	+1.316337	+34.000000	+1.700
+1.31250	+1.01677	+1.228944	+1.321304	+34.000000	+1.700
+1.37500	+1.01110	+1.206600	+1.319872	+34.000000	+1.700
+1.43750	+1.00453	+1.174906	+1.310125	+34.000000	+1.700
+1.50000	+0.98859	+1.195100	+1.313959	+34.000000	+1.700
+1.56250	+0.999627	+1.167338	+1.315956	+34.000000	+1.700
+1.62500	+0.99679	+1.146823	+1.316090	+34.000000	+1.700
+1.68750	+0.990239	+1.143553	+1.312369	+34.000000	+1.700
+1.75000	+0.98069	+1.075841	+1.311923	+34.000000	+1.700
+1.81250	+0.972236	+0.978715	+1.309808	+34.000000	+1.700
+1.87500	+0.97407	+0.936974	+1.310710	+34.000000	+1.700
+1.93750	+0.97314	+0.900165	+1.310005	+34.000000	+1.700
+2.00000	+1.100405	+1.002721	+1.317999	+34.000000	+1.700

The cascade loss coefficient based on initial dynamic pressure as calculated using mass averaged quantities as shown below.

$P_{t1} - P_{t2} = 51.7056530157 \text{ PSIA}$   
 $P_{t1} - P_{t2} = 50.4993345376 \text{ PSIA}$   
 $P_{t1} - P_{t2} = 30.1956451808 \text{ PSIA}$   
 $T_{avg} = 514.5 \text{ deg R}$   
 $W_{bar} = .084206392182$

Figure F1. (cont) Run 2 2/24/94 Raw Data

Data Print Out for Zoo # 1, Run # 4, File 201416744  
 Period between samples (sec): .0030303030303  
 Sample collection rate (Hz): 330  
 Number of samples per port: 10  
 Length of data run (sec): 31  
 The scan type is: 3  
 Number of scans/inverse-scan: 33  
 Increment of Inverse-scan: .0025 Inverse  
 Atmospheric pressure (at): 14.715 psia  
 Tunnel Pressure Ratio (at): 2.09427170669

Scan	Port Number					
	1	24	25	29	30	31
1	15.097	46.494	44.782	15.312	37.069	62.911
2	15.140	46.542	44.301	15.222	32.159	62.930
3	15.053	46.420	44.253	15.277	32.129	62.957
4	15.042	46.248	43.984	15.207	32.010	62.994
5	15.195	46.227	43.941	15.302	32.190	63.020
6	15.086	46.112	43.709	15.272	32.079	63.079
7	15.075	46.190	43.936	15.202	32.109	62.979
8	15.107	46.246	43.959	15.312	32.129	62.930
9	15.107	46.160	43.760	15.202	32.099	62.994
10	15.075	46.045	43.658	15.242	32.070	62.956
11	15.031	45.921	43.590	15.292	32.059	62.759
12	15.107	46.017	43.694	15.292	32.040	62.866
13	15.031	46.190	43.779	15.202	32.030	62.893
14	15.006	46.179	43.466	15.262	32.019	62.747
15	15.075	44.345	41.500	15.252	31.970	62.975
16	15.031	46.205	39.478	15.202	31.979	62.975
17	15.064	37.059	37.165	15.302	31.990	62.939
18	15.140	41.205	41.020	15.292	32.040	62.940
19	15.129	45.442	44.694	15.282	31.998	62.939
20	15.107	45.892	44.745	15.282	31.950	62.902
21	15.107	45.921	44.783	15.282	31.998	62.939
22	15.129	45.844	44.773	15.292	32.040	62.704
23	15.053	45.691	44.792	15.292	31.960	62.949
24	15.140	45.853	44.939	15.302	31.990	62.920
25	15.107	45.556	44.707	15.282	31.900	62.930
26	15.107	45.490	44.869	15.323	31.950	62.930
27	15.053	45.403	45.000	15.292	31.910	62.939
28	15.064	45.375	44.971	15.312	31.860	63.011
29	15.009	45.376	45.075	15.312	31.820	62.902
30	15.097	45.355	45.141	15.202	31.900	62.975
31	15.107	45.346	45.320	15.302	31.860	62.993
32	15.104	45.375	45.555	15.302	31.860	62.911
33	15.086	45.231	45.546	15.302	31.850	62.793

Figure F2. Run 4 2/24/94 Raw Data

Position	Beta	Gamma	Delta	Epsilon	Theta
+0.00000	+1.06918	+4.407285	+335743	+33.439332	+3.548
+0.06250	+1.07439	+4.40984	+337187	+33.356166	+3.512
+0.12500	+1.06877	+4.401589	+335075	+33.454211	+3.445
+0.18750	+1.07847	+4.437265	+336180	+33.174589	+4.072
+0.25000	+1.07011	+4.423172	+336001	+33.195039	+3.977
+0.31250	+1.04200	+4.444342	+326237	+33.070155	+4.100
+0.37500	+1.03900	+4.462525	+327415	+33.1790172	+4.233
+0.43750	+1.03921	+4.457537	+327471	+33.001073	+4.324
+0.50000	+1.04520	+4.457256	+328117	+33.013029	+4.341
+0.56250	+1.04380	+4.455215	+328733	+33.156270	+4.299
+0.62500	+1.04488	+4.446434	+329029	+33.468191	+4.147
+0.68750	+1.04038	+4.445915	+327794	+33.531022	+4.122
+0.75000	+1.03950	+4.463457	+327553	+33.748783	+4.438
+0.81250	+1.04172	+4.520485	+328161	+33.579769	+4.504
+0.87500	+0.98681	+4.599904	+309411	+33.523559	+6.705
+0.93750	+0.79337	+4.534907	+270226	+33.801343	+5.317
+1.00000	+0.42896	+4.411459	+192636	+34.331537	+3.003
+1.06250	+0.06499	+4.046222	+250035	+35.228939	+1.056
+1.12500	+0.94875	+4.179722	+303954	+35.426323	+0.090
+1.18750	+1.02192	+4.222420	+322777	+34.344859	+0.689
+1.25000	+1.02727	+4.219231	+324219	+34.265020	+0.628
+1.31250	+1.01532	+4.209210	+320999	+34.465525	+1.487
+1.37500	+1.01325	+4.176241	+320444	+34.454296	+1.050
+1.43750	+1.01580	+4.159021	+321127	+34.400583	+1.170
+1.50000	+1.01350	+4.168822	+320512	+34.369056	+0.949
+1.56250	+1.00172	+4.123711	+317386	+34.624414	+0.726
+1.62500	+1.00061	+4.080332	+317094	+34.662676	+1.175
+1.68750	+1.00457	+4.079940	+318137	+34.566758	+1.185
+1.75000	+0.99596	+4.059878	+315874	+34.765883	+1.429
+1.81250	+1.00239	+4.044425	+317553	+34.668833	+1.633
+1.87500	+0.99511	+4.005189	+315652	+34.665673	+2.121
+1.93750	+0.98856	+4.038082	+313950	+35.091164	+2.563
+2.00000	+0.99613	+4.062773	+315918	+34.889373	3.004

The cascade loss coefficient based on inlet dynamic pressure as calculated using mass averaged quantities as shown below.

P1a1 = 52.8913362148 PSIA  
P1a2 = 49.7055979741 PSIA  
P11-P1 = 37.6061847212 PSIA  
T1avg = 513 deg R  
W\_bar = .0047131241109

Figure F2. (cont) Run 4 2/24/94 Raw Data

Data Print Out for Zoc # 1 , Run # 5 , FileZR1414245  
 Period between samples (sec): .0030303030303  
 Sample collection rate (Hz): 330  
 Number of samples per port: 10  
 Length of data run (sec): 31  
 The scan type is: 4  
 Number of scans/traverses: 33  
 Increment of traverse: .0625 Inches  
 Atmospheric pressure is: 14.71 psia  
 Tunnel Pressure Ratio is: 2.1263124713

Scan	Port Number							
	01	24	25	29	30	31		
1	14.950	46.017	43.032	14.931	31.747	52.292	50.367	
2	14.901	45.873	43.537	14.991	31.762	52.271	50.100	
3	14.890	45.576	43.185	14.961	31.677	52.290	49.701	
4	14.880	45.643	43.299	15.001	31.717	52.319	49.548	
5	14.858	45.518	43.109	14.961	31.667	52.319	49.559	
6	14.880	45.681	43.223	14.991	31.707	52.319	49.617	
7	14.814	45.614	43.214	15.001	31.677	52.301	49.681	
8	14.880	45.768	43.280	14.971	31.635	52.237	49.897	
9	14.803	45.682	43.214	14.931	31.595	52.191	49.607	
10	14.782	45.624	42.937	14.991	31.646	52.209	49.395	
11	14.880	45.182	42.354	15.041	31.667	52.273	49.051	
12	14.847	43.819	41.089	15.011	31.656	52.264	47.054	
13	14.880	41.840	39.204	14.981	31.646	52.301	44.980	
14	14.869	39.783	37.904	14.981	31.677	52.301	42.012	
15	14.814	37.954	36.831	14.961	31.506	52.282	39.695	
16	14.869	37.259	36.537	14.921	31.687	52.292	39.568	
17	14.782	38.152	37.826	15.011	31.586	52.292	39.998	
18	14.825	40.715	40.501	14.951	31.536	52.118	43.491	
19	14.835	43.348	42.718	14.931	31.576	52.246	47.425	
20	14.880	44.826	44.059	14.971	31.667	52.256	49.396	
21	14.858	45.326	44.211	14.971	31.626	52.285	49.887	
22	14.890	45.326	44.316	14.961	31.616	52.191	49.964	
23	14.912	45.288	44.211	15.021	31.566	52.118	49.964	
24	14.880	45.345	44.240	14.971	31.616	52.319	50.040	
25	14.869	45.269	44.202	15.001	31.596	52.293	49.897	
26	14.901	45.249	44.259	14.991	31.636	52.264	49.848	
27	14.912	45.269	44.230	14.981	31.556	52.285	49.916	
28	14.869	45.230	44.240	14.991	31.596	52.264	49.910	
29	14.836	44.999	44.192	14.981	31.606	52.346	49.627	
30	14.901	44.961	44.325	15.001	31.546	52.319	49.694	
31	14.956	44.990	44.675	15.051	31.667	52.401	49.858	
32	14.901	44.913	44.897	15.061	31.536	52.200	49.973	
33	14.912	44.711	45.053	15.011	31.566	52.209	49.983	

Figure F3. Run 5 2/24/94 Raw Data

Position	Beta	Gamma	X (μ)	Y (μ)	6.4° - θ
+0.00000	+1.00001	+1.001499	+1.330000	+1.330000	+1.0000
+1.17500	+1.007031	+1.005216	+1.330044	+1.330044	+1.0000
+1.25000	+1.007102	+1.005102	+1.330050	+1.330050	+1.0000
+1.37500	+1.004235	+1.005942	+1.330233	+1.330233	+1.0000
+1.50000	+1.005448	+1.005006	+1.331700	+1.331700	+1.0000
+1.67500	+1.004002	+1.005026	+1.332000	+1.332000	+1.0000
+1.65625	+1.006001	+1.005454	+1.333420	+1.333420	+1.0000
+1.68750	+1.007499	+1.005900	+1.333540	+1.333540	+1.0000
+1.71875	+1.004209	+1.005635	+1.330263	+1.330263	+1.0000
+1.75000	+1.003370	+1.002647	+1.329060	+1.329060	+1.0000
+1.78125	+1.003999	+1.004629	+1.327600	+1.327600	+1.0000
+1.81250	+1.000007	+1.000371	+1.316630	+1.316630	+1.0000
+1.84375	+1.006630	+1.000125	+1.300200	+1.300200	+1.0000
+1.87500	+1.006300	+1.000406	+1.264307	+1.264307	+1.0000
+1.90625	+1.005793	+1.007907	+1.272000	+1.272000	+1.0000
+1.93750	+1.004329	+1.002427	+1.193573	+1.193573	+1.0000
+1.96875	+1.005022	+1.002106	+1.200723	+1.200723	+1.0000
+1.00000	+1.002670	+1.004027	+1.244407	+1.244407	+1.0000
+1.03125	+1.002627	+1.144428	+1.200607	+1.200607	+1.0000
+1.06250	+1.000906	+1.153376	+1.110097	+1.110097	+1.0000
+1.09375	+1.002500	+1.017040	+1.323945	+1.323945	+1.0000
+1.12500	+1.002920	+1.196521	+1.324763	+1.324763	+1.0000
+1.15625	+1.104194	+1.206036	+1.320193	+1.320193	+1.0000
+1.18750	+1.104071	+1.210690	+1.330003	+1.330003	+1.0000
+1.21875	+1.103263	+1.207073	+1.325674	+1.325674	+1.0000
+1.25000	+1.102192	+1.194471	+1.322773	+1.322773	+1.0000
+1.28125	+1.103496	+1.200091	+1.326310	+1.326310	+1.0000
+1.31250	+1.101802	+1.195161	+1.321930	+1.321930	+1.0000
+1.34500	+1.101374	+1.160414	+1.320575	+1.320575	+1.0000
+1.38750	+1.101646	+1.125009	+1.321303	+1.321303	+1.0000
+1.42750	+1.100792	+1.062604	+1.310075	+1.310075	+1.0000
+1.46250	+1.100422	+1.016691	+1.310046	+1.310046	+1.0000
+1.00000	+1.102052	+1.067175	+1.322395	+1.322395	+1.0000

Figure F3. (cont) Run 5 2/24/94 Raw Data

## LIST OF REFERENCES

1. McCormick, D., "Shock-Boundary Layer Interaction Control with Low-Profile Vortex Generators and Passive Cavity", AIAA Paper 92-0064, January 1992.
2. United Technologies Research Center Report R90-957946-13, Transonic Fan Shock Boundary Layer Separation Control, April 1990.
3. Collins, C., Preliminary Investigation of the Shock-Boundary Interaction in a Simulated Fan Passage, M.S.A.E. Thesis, Naval Postgraduate School, Monterey, California, March 1991.
4. Golden, W., Static Pressure Measurements of the Shock-Boundary Layer Interaction in a Simulated Fan Passage, M.S.A.E. Thesis, Naval Postgraduate School, Monterey, California, March 1992.
5. Myre, D., Model Fan Passage Flow Simulation, M.S.A.E. Thesis, Naval Postgraduate School, Monterey, California, December 1992.
6. Tapp, E., Development of a Cascade Simulation of a Fan-Passage Flow, M.S.A.E. Thesis, Naval Postgraduate School, Monterey, California, December 1993.
7. AGARD-AG-207, Modern Methods of Testing Rotating Components of Turbomachines (Instrumentation), by Sieverding, C., 1975.
8. Geopfarth, R., Development of a Device for the Incorporation of Multiple Scanvalves into a Computer-Controlled Data System, M.S.A.E. Thesis, Naval Postgraduate School, Monterey, California, March 1979.
9. Neuhoﬀ, F., Calibration and Application of a Combination Temperature-Pneumatic Probe for Velocity and Rotor Loss Distribution Measurements in a Compressor, BDM Corporation, Contractor Report, December 1981.
10. Nakamura, S., Applied Numerical Methods with Software, Prentice-Hall, Inc., Englewood Cliffs, New Jersey, 1991.
11. Holman, J., Experimental Methods for Engineers, Fifth Edition, McGraw-Hill, Inc., 1989.
12. Armstrong, J., Near-Stall Loss Measurements in a CD Compressor Cascade with Exploratory Leading Edge Flow Control, M.S.A.E. Thesis, Naval Postgraduate School, Monterey, California, June 1990.

13. Shreeve, R., Elazar, Y., Dreon, J., and Baydar, A., "Wake Measurements and Loss Evaluation in a Controlled Diffusion Compressor Cascade", Transactions of the ASME, Journal of Turbomachinery, Vol. 113, No. 4, pp. 591-599, October 1991.

## INITIAL DISTRIBUTION LIST

- |   |         |
|---|---------|
| 1. Defense Technical Information Center<br>Cameron Station<br>Alexandria, Virginia 22304-6145   | 2       |
| 2. Library, Code 52<br>Naval Postgraduate School<br>Monterey, California 93943-5002   | 2       |
| 3. Department of Aeronautics and Astronautics<br>Naval Postgraduate School<br>Monterey, California 93943-5002<br>ATTN: Chairman<br>ATTN: Code AA/SF | 1<br>10 |
| 4. Commanding Officer<br>Naval Aircraft Warfare Center<br>Aircraft Division<br>Trenton, New Jersey 08628-0176<br>ATTN: S. Clouser                   | 1       |
| 5. Naval Air Systems Command<br>Washington, D.C. 20361<br>ATTN: AIR-536T  | 1       |
| 6. Office of Naval Research<br>800 North Quincy Street<br>Arlington, Virginia 22217<br>ATTN: Spiro Lykoudis   | 1       |
| 7. United Technologies Research Center<br>East Hartford, Connecticut 06108<br>ATTN: Duane McCormick   | 1       |
| 8. Lt. Jeff Austin<br>Operations Department<br>USS Carl Vinson (CVN-70)<br>FPO AP 96629-2840  | 2       |

DUDLEY KNOX LIBRARY  
NAVAL POSTGRADUATE SCHOOL  
MONTEREY CA 93943-5101



GAYLORD S

DUDLEY KNOX LIBRARY



3 2768 00018801 5